



LUND UNIVERSITY

Nanotools for biosensing and manipulating cells

Johansson, Therese

2024

[Link to publication](#)

Citation for published version (APA):

Johansson, T. (2024). *Nanotools for biosensing and manipulating cells*. Department of Physics, Lund University.

Total number of authors:

1

General rights

Unless other specific re-use rights are stated the following general rights apply:

Copyright and moral rights for the publications made accessible in the public portal are retained by the authors and/or other copyright owners and it is a condition of accessing publications that users recognise and abide by the legal requirements associated with these rights.

- Users may download and print one copy of any publication from the public portal for the purpose of private study or research.
- You may not further distribute the material or use it for any profit-making activity or commercial gain
- You may freely distribute the URL identifying the publication in the public portal

Read more about Creative commons licenses: <https://creativecommons.org/licenses/>

Take down policy

If you believe that this document breaches copyright please contact us providing details, and we will remove access to the work immediately and investigate your claim.

LUND UNIVERSITY

PO Box 117
221 00 Lund
+46 46-222 00 00



Nanotools for biosensing and manipulating cells

THERESE JOHANSSON

DEPARTMENT OF PHYSICS | FACULTY OF ENGINEERING | LUND UNIVERSITY



Nanotools for biosensing and manipulating cells

Nanotools for biosensing and manipulating cells

Therese Johansson



LUND
UNIVERSITY

DOCTORAL DISSERTATION

Doctoral dissertation for the degree of Doctor of Philosophy (PhD) at the Faculty of Engineering at Lund University to be publicly defended on Friday January 12th 2024 at 09.15 in Rydbergsalen, Department of Physics, Sölvegatan 14

Faculty opponent

Professor Pawel Sikorski, Norwegian University of Science and Technology

Organization: LUND UNIVERSITY

Document name: Doctoral Thesis

Date of issue: 2024-01-12

Author(s): Therese Johansson

Sponsoring organization:

Title and subtitle: Nanotools for biosensing and manipulating cells

Abstract:

In medical research and within the field of Biology, it is important to find effective tools for probing and manipulating cells, as well as tools for detecting biomolecules. These tools should be sensitive, with high specificity, and, if aimed at interacting with cells, they should be minimally invasive. In this thesis, I investigated the potential of various nanotools for these purposes. Specifically, I investigated the use of photovoltaic nanowires as a tool to manipulate cancer cells and send them to dormancy. I also evaluate the potential of using molecular beacons to sense the transcriptional state of cells with respect to a specific gene, and to detect oligonucleotides in solution. The work has been divided into three projects.

Apart from the normal cell division cycle, where cells normally prepare for division, they can also enter a dormant state. Many cancer treatments aim to kill the cancer cells at specific steps in the cell division cycle. If the cancer cells then are dormant, they can evade the treatment, resulting in reoccurring cancer and metastasis. This reveals a need for a cell dormancy switch, where cells can be forced to enter dormancy in a controlled way in vitro. This would enable further investigation of dormancy in cells, and make it possible to study how dormant cells react to new potential treatments. Nanowires are high aspect ratio nanostructures, which are today mainly used in optoelectronic nanodevices. In this thesis, I show that cells seeded on InP p-i-n nanowires can enter dormancy when they are illuminated. This makes the setup act as a cell dormancy switch. Through control experiments, I could conclude that the induced dormancy was due to injection of carriers into the medium surrounding the nanowires. In this thesis, I also investigate whether molecular beacons can be used to probe for *Ins-1* mRNA, and for measuring its concentration inside of beta cells. Molecular beacons are hairpin shaped chains of nucleic acids, with a loop sequence designed to be complementary to the specific mRNA of interest. In order for molecular beacons to report the presence of mRNA in cells, they need to be injected in the cytosol. Nanostraws were used for this purpose. Nanostraws are hollow alumina nanotubes, that can be used together with electrical pulses to inject cargo into cells. In the second project of the thesis, molecular beacons were injected to a large number of beta cells using nanostraws and the beacon signal inside cells was monitored over time using fluorescence microscopy. The results show that when the molecular beacons enter the cell, they seem to be degraded, resulting in false positive signal. This makes the assessment of mRNA in cells challenging with this method.

In a third project, I show that molecular beacons can be used as a probe for oligonucleotides in solution. To amplify the molecular beacon signal upon hybridization, beacons were immobilized on light guiding nanowires in a microchannel. Complementary oligonucleotides were added in the microchannel over the nanowires and could be detected with a limit of detection of 0.1 nM, making the setup a promising alternative to current probing methods.

Key words: Biosensing, molecular beacons, cancer cells, dormancy, beta cells, nanowires, light guiding, nanostraws, fluorescence

Classification system and/or index terms (if any)

Supplementary bibliographical information

Language English

ISSN and key title:

ISBN: 978-91-8039-809-1 (print)

978-91-8039-810-7 (electronic)

Recipient's notes

Number of pages: 87

Price

Security classification

I, the undersigned, being the copyright owner of the abstract of the above-mentioned dissertation, hereby grant to all reference sources permission to publish and disseminate the abstract of the above-mentioned dissertation.

Signature

Date 2023-11-27

Nanotools for biosensing and manipulating cells

Therese Johansson



LUND
UNIVERSITY

Coverphoto by Therese Johansson
Back cover photographer: Sara Davidsson Bencker
Copyright i-67 Therese Johansson

Paper I © by the Authors (Manuscript published)
Paper II © by the Authors (Manuscript submitted)
Paper III © by the Authors (Manuscript unpublished)

Division of Solid State Physics
Department of Physics
Faculty of Engineering
Lund University

ISBN 978-91-8039-809-1 (print)
ISBN 978-91-8039-810-7 (electronic)

Printed in Sweden by Media-Tryck, Lund University
Lund 2024



Media-Tryck is a Nordic Swan Ecolabel certified provider of printed material. Read more about our environmental work at www.mediatryck.lu.se

MADE IN SWEDEN 

Dedicated to Karl-Johan

Table of Contents

Abstract	i
Populärvetenskaplig sammanfattning	iii
Acknowledgements	v
List of Papers.....	vii
Abbreviations	ix
1 Introduction	1
1.1 Interactions between cells and 1D structures.....	1
1.1.1 Effects on cell adhesion, viability, motility and morphology...	1
1.1.2 Membrane-NW interactions in the context of cell transfection	3
1.1.3 Transfection using nanostraws	4
1.1.4 Nanowires for biosensing	5
1.2 Detection of mRNA.....	7
1.3 My contribution	9
1.4 Outline of thesis.....	10
2 Photovoltaic NWs as dormancy switch (project 1).....	11
2.1 Background.....	11
2.1.1 Cell cycle and dormancy	11
2.1.2 Function of photovoltaic NWs	12
2.2 Results	14
2.2.1 Characterization of the NWs	14
2.2.2 Effect of illumination on cells seeded on p-i-n NWs.....	16
3 Detection of <i>Ins1</i> mRNA using MBs and nanostraws (project 2)	21
3.1 Background.....	21
3.1.1 mRNA detection in cells.....	21
3.1.2 Structure and function of MBs	21
3.1.3 Challenges when designing suitable MBs	22
3.1.4 MBs in cells.....	23
3.1.5 Nanostraws for intracellular delivery	24
3.2 Results	24
3.2.1 Functionality of MBs.....	24
3.2.2 Cell viability after intracellular delivery of MBs.....	25
3.2.3 Monitoring insulin mRNA using <i>Ins1</i> MBs	26

3.2.4	Fate of <i>InsI</i> MBs in cells in time and space	27
3.2.5	Scrambled MBs as control for specificity	28
4	Detection of oligonucleotides using MBs immobilized on light guiding NWs (project 3).....	31
4.1	Background.....	31
4.1.1	Immobilization of MBs	31
4.1.2	Limit of detection (LOD)	31
4.1.3	Lightguiding NWs	32
4.2	Results	33
4.2.1	Functionality of NWs	33
4.2.2	Detection of complementary oligonucleotides on the NW platform	34
5	Experimental methods	39
5.1	NW synthesis and characterization.....	39
5.1.1	Metalorganic vapor phase epitaxy (MOVPE)	39
5.1.2	Atomic layer deposition (ALD).....	40
5.1.3	Scanning electron microscopy (SEM).....	41
5.1.4	Electron beam-induced current (EBIC).....	42
5.2	Cells.....	42
5.2.1	Cell culture	43
5.2.2	Illumination of cells and photovoltaic NWs.....	43
5.3	Nanostraws	43
5.3.1	Nanostraw fabrication.....	44
5.3.2	Nanoelectroporation	44
5.4	Fluorescence	45
5.4.1	Fluorescence microscopy	45
5.4.2	Fluorescence labelling	46
5.4.3	Fluorescence plate reader measurements.....	48
5.4.4	Flow cytometry.....	49
5.5	Molecular beacons.....	50
5.5.1	MB design	50
5.5.2	Immobilization of MBs	50
5.6	Data analysis.....	51
6	Concluding remarks and Outlook	53
6.1	Photovoltaic NWs as dormancy switch.....	53
6.2	Detection of <i>InsI</i> mRNA using MBs and nanostraws.....	54
6.3	Detection of oligonucleotides using MBs immobilized on light guiding NWs	55
7	References	57

Abstract

In medical research and within the field of Biology, it is important to find effective tools for probing and manipulating cells, as well as tools for detecting biomolecules. These tools should be sensitive, with high specificity, and, if aimed at interacting with cells, they should be minimally invasive. In this thesis, I investigated the potential of various nanotools for these purposes. Specifically, I investigated the use of photovoltaic nanowires as a tool to manipulate cancer cells and send them to dormancy. I also evaluate the potential of using molecular beacons to sense the transcriptional state of cells with respect to a specific gene, and to detect oligonucleotides in solution. The work has been divided into three projects.

Apart from the normal cell division cycle, where cells normally prepare for division, they can also enter a dormant state. Many cancer treatments aim to kill the cancer cells at specific steps in the cell division cycle. If the cancer cells then are dormant, they can evade the treatment, resulting in reoccurring cancer and metastasis. This reveals a need for a cell dormancy switch, where cells can be forced to enter dormancy in a controlled way in vitro. This would enable further investigation of dormancy in cells, and make it possible to study how dormant cells react to new potential treatments. Nanowires are high aspect ratio nanostructures, which are today mainly used in optoelectronic nanodevices. In this thesis, I show that cells seeded on InP p-i-n nanowires can enter dormancy when they are illuminated. This makes the setup act as a cell dormancy switch. Through control experiments, I could conclude that the induced dormancy was due to injection of carriers into the medium surrounding the nanowires.

In this thesis, I also investigate whether molecular beacons can be used to probe for *Ins1* mRNA, and for measuring its concentration inside of beta cells. Molecular beacons are hairpin shaped chains of nucleic acids, with a loop sequence designed to be complementary to the specific mRNA of interest. In order for molecular beacons to report the presence of mRNA in cells, they need to be injected in the cytosol. Nanostraws were used for this purpose. Nanostraws are hollow alumina nanotubes, that can be used together with electrical pulses to inject cargo into cells. In the second project of the thesis, molecular beacons were injected to a large number of beta cells using nanostraws and the beacon signal inside cells was monitored over time using fluorescence microscopy. The results show that when the molecular beacons enter the cell, they seem to be degraded, resulting in false positive signal. This makes the assessment of mRNA in cells challenging with this method.

In a third project, I show that molecular beacons can be used as a probe for oligonucleotides in solution. To amplify the molecular beacon signal upon hybridization, beacons were immobilized on light guiding nanowires in a

microchannel. Complementary oligonucleotides were added in the microchannel over the nanowires and could be detected with a limit of detection of 0.1 nM, making the setup a promising alternative to current probing methods.

Populärvetenskaplig sammanfattning

Inom medicin- och biologiforskningen är det viktigt att ha tillgång till verktyg för att undersöka och manipulera celler, samt även att på ett enkelt och smidigt sätt kunna detektera biomolekyler som inte befinner sig i en intakt levande cell. När det gäller verktyg för att undersöka och manipulera celler är det av stor vikt att dessa tekniker inte skadar cellerna eller påverkar deras funktion under behandlingen eller mätningen, samtidigt som hög precision önskas. Denna avhandling handlar om hur väldigt små strukturer (nanostrukturer), med dimensioner mindre än en tusendel av en hårstråsbredd, kan bidra till att utveckla sådana metoder. Detta presenteras som tre olika projekt.

Ett problem inom dagens cancerbehandling är att cancerceller kan gå in i viloläge, där de inte påverkas lika mycket av omgivningen och på så sätt lyckas undgå behandlingen. Detta leder till ökad risk att cancer kvarstår eller återkommer. Som ett led i att utveckla mer effektiva behandlingsmetoder är det av stor vikt att ha tillgång till metoder där cancerceller i viloläge kan studeras.

Det första projektet handlar därför om hur en speciell typ av små så kallade nanotrådar (som kan absorbera ljus och omvandla det till ström), kan användas som strömbrytare för att få celler att på ett kontrollerat sätt gå in i viloläge. Cancerceller odlades på nanotrådarna som sedan belystes under 48 timmar. Ljuset gjorde att strömbrytaren slogs på och cellerna ”somnade”. Slutsatsen från experimenten blev att den ström som uppstår i nanotrådarna när de belyses med ljus är det som påverkar cellerna.

Avhandlingens resterande två projekt siktar på att ta fram en effektivare teknik för att avläsa vilka proteiner som produceras i en cell och i vilken mängd. När en cell behöver ett speciellt protein, kopieras receptet som finns i vårt DNA för just detta protein. Kopierad kallas mRNA och det skickas ut till ribosomer, som är cellens proteinfabriker. För att förstå hur celler fungerar och reagerar i olika situationer är det viktigt att kunna mäta vilka mRNA som är i rörelse i cellen, och i vilka mängder dessa finns. Det finns idag flera metoder för att mäta detta. Några vanliga nackdelar med dessa metoder är dock att det krävs många celler, och att man får ett medelresultat för alla celler tillsammans istället för information om enskilda celler. Det är även vanligt att cellerna dör före eller under mätningen.

För att komma runt dessa nackdelar har vi använt en hårnålsliknande struktur (molecular beacons på engelska), uppbyggd av en kedja av de byggstenar som vanligen återfinns i DNA och RNA (nukleotider). Det finns fyra sorters nukleotider och de binder till varandra i specifika par. I dessa hårnålsstrukturer finns en kedja av nukleotider som bildar en stam och en ögla, eftersom nukleotider i motsatta ändar av kedjan binder till varandra som ett blixtlås och håller strukturen stängd. Blixtlåset går dock inte att stänga hela vägen upp, så det bildas en ögla med obundna nucleotider i toppen. I ena änden av kedjan sitter en molekyl som lyser, och i den

andra änden en molekyl som agerar ljussläckare. När de är nära varandra så släcks ljuset, men när hårnålsstrukturen öppnas når inte ljussläckaren längre och det skickas ut ljus. Som en del i denna avhandling undersöktes hur dessa molekulära hårnålsstrukturer skulle kunna användas för att spåra mRNA i celler. När hårnålsstrukturens ögla kommer i kontakt med ett matchande mRNA binder dessa till varandra och hårnålsstrukturen öppnas så att ljus sänds ut. Detta gör att öppning av strukturen kan mätas i till exempel ett mikroskop. Molekulära hårnålsstrukturer öppnas alltså av ett specifikt mRNA som cellen producerat, och på så sätt kan detta mRNA detekteras i en levande cell.

I avhandlingens andra projekt undersöktes huruvida ett mRNA som är förknippat med insulinproduktion kan detekteras inne i en cell. Genom tunna nanostrån som kan liknas vid väldigt små sugrör, injicerades specialdesignade molekulära hårnålsstrukturer in i många celler samtidigt med hjälp av en svag elektrisk spänning. När hårnålsfyren lyser upp blir det möjligt att undersöka dess öde inne i cellen, vart den tar vägen och om den faktiskt hittat sitt matchande mRNA, eller om den istället verkar brytas ner. Mycket talar för att hårnålsstrukturen till stor del bryts ner till sina beståndsdelar inne i cellen.

slutligen handlar avhandlingens tredje projekt om hur signal från de molekulära hårnålsstrukturerna kan förstärkas genom att förankra dem på ljusledande nanotrådar. Nanotrådarna placerades upp och ner i taket av en smal kanal där hårnålsstrukturerna sedan fastnade tack vare flera förankrande lager. Sedan kunde en förenklad kopia av hårnålsfyrens matchande mRNA (målmolekyl) pumpas genom kanalen och detekteras. Ljuset från enskilda hårnålsstrukturer som hittat sin målmolekyl leddes genom nanotråden och ut genom dess topp, likt en ficklampa. Tack vare de ljusledande nanotrådarna kunde låga koncentrationer av målmolekylen detekteras.

Acknowledgements

This PhD journey would not have been possible without the help and support of a lot of people. First of all, I want to thank my supervisor Christelle for the opportunity to join the Prinz group and for making me feel welcome since day one. I have learned so much about research, but also life in general from you. Thank you for your constant support.

Jonas T and Mercy, thank you for being my co-supervisors. Mercy, you taught me all I needed to know in the lab, and I am grateful for your patience and knowledge.

I would also like to thank current and former members of the Prinz group: Mercy, Elke, Laura, and Martin for welcoming me into the group, Diogo for sharing your knowledge and spirit, Mokhtar and Karthik for introducing new perspectives, and Frida for spreading joy and act as sanity check when the road sometimes got a bit bumpy. To Thea and Sara, who most recently joined the group, thank you for nice conversations, and I hope you will feel as welcome as I have in the group.

I also got the best office mate I could ever wish for. Thank you Esra for always being there during both good and less good times, and for always spreading joy around you. You are a great friend.

To the FTF biogroup people, thank you for interesting discussions and for always wanting to help when possible. A special thanks to the bacon gang, Julia and Ruby, for putting in so much work to reach our shining results, to Jason for practical help and feedback during my work, and to Pradheebha and Vanya for sharing this PhD experience with me from the very start. Thank you also Elham, Enrico, Mariia, and Patrik. From outside the biogroup, thank you Florinda, Steffen, Stephanie, Simon, Max, Antti, Asmita, Thanos, David A, Kristi, Linnéa, Markus A, Markus S, Sara, Anette, and all others for nice corridor discussions.

When doing a PhD, there is so much more than just the science part that needs to work. Thank you to all administrative and supporting staff for always helping out. To Alexandra, Anna, Mia, Charlotte, Marica, Gerda, Gabriele, Anastasiia, Anna-Karin, Mirja, Evelina, Anneli, Anders G, Johanna, Alfons, Andreas, George, Håkan, Natalia, Alexander, Emil, Anders K, Peter, Sarah, and Bengt. Thank you to Luke, Maria H, and Dan for showing great and human leadership. To Adam for guidance through the thesis and defense process. To Karin and Britta for always being positive and nice. To Martin A for good mentorship, and then not to forget, all the members of LTHooked.

I also had the pleasure to be involved in undergraduate education within my PhD. Thank you to Maria M, Magnus, Carina, Jonas J, Charlotta, Tommy, and Claes-Göran for inspiration and for helping me develop my teaching skills.

During the years, I also have had the possibility to be involved in different collaborations. An extra thank you to Roberto for all the help with designing the molecular beacons, and to Kush for sharing your experiences about company work. Thank you also Heiner for collaboration in Genes & Wires project, Fredrik, Adrian and Björn at Chalmers, Sara and Mattias at biochemistry department, and Christopher and Marco at Physical chemistry.

To all of you that are not mentioned above, but who has in any way contributed to make my PhD journey a bit easier, either practically or just by creating a nice working environment, thank you all.

Also outside of work, I would like to thank Lena, Aron, Ally, Thomas Jenny L, my parents and siblings, and many more for inspiration and support. Then of course, my dearest Karl-Johan. Without you, there would be nothing. Thank you for always being my biggest supporter, no matter what.

List of Papers

This thesis is based on the following papers. Due to a name change during my PhD studies, I am listed with two different surnames, Olsson and Johansson.

Paper I

Photovoltaic nanowires affect human lung cell proliferation under illumination conditions

Therese B. Olsson, Laura Abariute, Lukas Hrachowina, Enrique Barrigón, Diogo Volpati, Steven Limpert, Gaute Otnes, Magnus T. Borgström and Christelle N. Prinz.

Nanoscale, 2020, 12, 14237

I further developed previously existing experimental protocols and designed new experiments, with focus on controls and follow-ups to the main experiment. I did the experimental part together with L. Abariute, including cell culturing, light/dark dormancy experiments and analysis. I wrote the manuscript together with co-authors.

Paper II

Using molecular beacon fluorescence in cells for mRNA detection: the challenge of false positive signals

Diogo Volpati, Pedro H. B. Aoki, Therese B. Johansson , Roberto Munita, Frida Ekstrand, Sabrina Ruhrmann, Karl Bacos, Charlotte Ling, Christelle N. Prinz

Submitted

I participated in the discussions about experimental design. I performed all plate reader measurements and analysis connected to this. I did cell culturing, nanoelectroporation, cell labelling, fluorescence microscopy of the injected cells, and data analysis, everything together with D. Volpati, C.N. Prinz, and P.H.B. Aoki. I contributed to the writing of the manuscript.

Paper III

Sub nanomolar detection of oligonucleotides using molecular beacons immobilized on light guiding nanowires

Therese B. Johansson, Rubina Davtyan, Julia Valderas-Gutiérrez, Adrian Gonzalez Rodriguez, Björn Agnarsson, Roberto Munita, Heiner Linke, Fredrik Höök, Christelle N. Prinz

In manuscript

I designed the experiment together with co-authors. I did all plate reader measurements and analysis connected to this. I performed the MB immobilization and together with R. Davtyan and J. Valderas-Gutiérrez, I run the fluorescence experiments and participated in the data analysis. I wrote the manuscript together with C.N. Prinz and with input from co-authors.

Abbreviations

Frequently used:

MBs	Molecular beacons
NWs	Nanowires

All abbreviations:

ALD	Atomic layer deposition
ANOVA	Analysis of variance
DEZn	Diethylzink
DTL	Displacement Talbot lithography
DPBS	Dulbecco's phosphate buffered saline
EBIC	Electron beam-induced current
FBS	Fetal bovine serum
GaP	Gallium phosphide
ICP-RIE	Inductively coupled plasma and reactive ion etching
IDT	Integrated DNA Technologies
InP	Indium phosphide
LED	Light emitting diode
LNL	Lund nano lab
MBs	Molecular beacons
MOVPE	Metalorganic vapor phase epitaxy
NWs	Nanowires
PC	Polycarbonate
PDMS	polydimethylsiloxane
PFA	Paraformaldehyde
PH ₃	Phosphine
PLL-g-PEG	Poly-L-Lysine grafted Polyethylene Glycol
PS	Phosphorothioate
ROI	Region of interest
SEM	Scanning electron microscopy
TESn	Tetraethyltin
TEGa	Trimethylgallium
TMIn	TrimethylIndium
TUNEL	Terminal deoxynucleotidyl transferase dUTP nick end labeling

1 Introduction

From a biology and biomedicine point of view, it is important to gain the ability to probe and manipulate cells, for instance to investigate cell function and diseases. Cell manipulation includes stimulating or blocking certain mechanisms, using for instance chemical interactions, topography-mediated interactions, mechanotransduction, and transfection. In order to probe cells, one can use optical fluorescence microscopy and determine a variety of cell properties, such as morphology, proliferation and motility. An important parameter when investigating cells is the change in the transcriptional state of the cells after cell manipulation. Ideally, cell probing should avoid killing the cells, in order to allow for longitudinal studies. Therefore, the detection of mRNA in living cells is valuable. To tackle these challenges, an important aspect is to develop tools that are non-invasive and interfere as little as possible with the cell behaviour. Among the possible tools being explored, molecular beacons (MBs) and nanostructures, such as nanostraws and nanowires (NWs) are interesting candidates. Below is an introduction of the interactions between 1D nanostructures and cells, as well as an introduction to the most commonly used techniques to probe mRNA in cells.

1.1 Interactions between cells and 1D structures

Studies of the interactions between cells and different 1D nanostructures is of great importance to investigate the effects of these nanostructures on the cells, but also to develop and optimize platforms and tools for cell culturing, biosensing, and cell manipulation. Many 1D nanostructure parameters, such as size and density, affect the cell-nanostructure interactions.

1.1.1 Effects on cell adhesion, viability, motility and morphology

Adhesion and viability of cells are examples of parameters used to evaluate the biocompatibility of 1D structures. Nanowire substrates have been shown to work well as cell culture substrates [1], [2]. Results from neurons seeded on 2.5 μm long GaP NWs demonstrate that the NW substrate supports cell adhesion and axonal growth. The viability of the cells was better on GaP NWs compared to cells seeded on flat

GaP or glass [3]. When seeding HEK293 cells and neurons on 1-3 μm long InAs NWs, multiple critical functions in the cells were not impaired by the NW presence, supporting the hypothesis that NW arrays in general are not invasive to cells [4]. Comparing HEK293 cells seeded on 4.4 μm μm InAs NWs and on a flat glass surface, it was demonstrated that cells on NWs have an increased adhesion to the array, due to physical entrapment of the cells, but also an upregulation of the focal adhesion of the cells [5]. A recent study of NIF-3T3 fibroblasts seeded on 1 μm long SU-8 nanopillar arrays showed that the adhesion of the cells was affected by the pitch of the array, which was varied from 0.75 μm to 10 μm . The results showed that fibroblasts seeded on nanopillars with a pitch of 1 μm or less remained on the top of the pillars, with very little contact with the glass substrate. On arrays with pitches of 2 μm or more however, the cells could be seen in close contact with the nanopillar and also attached to the glass surface in between [6]. These results on the positioning of cells are in agreement with a later study seeding U2SOS cells on SU-8 nanopillar arrays of different pitches ranging from 0.5 μm to 2 μm and with a pillar length of 0.5 μm or 1 μm . The cells could then be divided into three categories: cells positioned at the top of the pillars for dense arrays, cells adhering to the nanopillars mostly at the cell edges for intermediate array densities, and cells in contact with the underlying glass substrate for sparse arrays [7].

Different levels of adhesion of the cells to the 1D structures may also affect the motility of the cells. In the fibroblasts on SU-8 nanopillars study mentioned above, the positioning of the cell on the different pitch arrays resulted in a lower migration rate for cells on high pitch arrays, which the authors suggest is due to strong contact between the cell and the glass as well as an engulfment of the nanopillars [6]. This decrease in mobility was also observed when L929 fibroblasts were seeded on 3.9 μm long GaP nanowires with a density of 0.1 NW per μm^2 and 1 NW per μm^2 . In that study, the cells seeded on the lower density substrates were completely immobile, whereas when seeded on NWs with higher density (4 NWs per μm^2), the mobility was comparable with cells seeded on flat polystyrene or flat GaP surfaces. The higher NW density was then considered to act as a bed-of-nails, facilitating the cell migration compared to lower NW densities [8]. Impairment of the cell motility and cell division can also be due to increasing NW length, as observed for instance in L929 fibroblasts seeded on GaP NWs of 1 μm^{-2} density and with length varying from 1.5 μm of up to 6.7 μm [9]. In that study, culturing L929 on 6.7 μm long NWs gave the more pronounced effect with completely immobilized cells on the NWs.

Cells are also affected differently in terms of morphology when seeded on NW arrays with different NW spacing. HEK293 cells cultured for 48 hours on a NW array with high NW density (29 NWs/100 μm^2) shows a more rounded morphology than the same cells cultured on lower NW densities (1-5 NWs/100 μm^2), which adopt a more flat appearance. As a consequence, a decreased cell area was observed for increased NW density [5]. This could also be seen in a later study, where the

effects of GaP NW array topography on MCF7 and MCF10A cells were investigated. The cell size was observed to be smaller for cells seeded on the NWs compared to cells seeded on flat GaP, and the cell area decreased when increasing the NW density [10].

Altogether, these results point at the importance of the design of 1D structures for interfacing cells. Due to their high aspect ratio morphology, at an early stage of the NW-cell research, there were thoughts that NWs might be able to be used for transfecting cells, as described below.

1.1.2 Membrane-NW interactions in the context of cell transfection

By depositing biomolecules on silicon NWs coated with aminosilane, Shalek *et al.* suggested that this NW platform can be used to transfect a variety of cells with any type of biomolecules [11]. Cells were cultured for 24h on the NW platform with e.g. predeposited Alexa Fluor 546 labelled siRNA, Rhodamine labelled peptides, or Cy5 labelled plasmid DNA. Cells were then transferred to a glass surface, and fluorescence microscopy showed fluorescence signal from what appear to be from inside the cells. Several studies demonstrating the applicability of the methods followed [12]–[14]. Later research could however show that similar results could be obtained by seeding cells directly on a glass surface coated with a biomolecule [15]. In that study, a NW device, intended to work as an inexpensive and cell compatible NW impalement device, was used to study the cell-NW interactions, in that case HeLa cells and HEK293 cells on copper oxide NWs. Using TEM and fluorescence microscopy, it was shown that the NWs did not penetrate the cell membrane, but instead the membrane wrapped tightly around the NWs. This suggests that biomolecules ending up inside cells are not introduced by direct transfection from the NWs, which is also supported by other research groups, using confocal z-stack imaging and optimized cell membrane labelling for HEK293 cells on InAs NWs [16], and using focused ion beam milling and SEM for L929 fibroblasts on GaP NWs [9].

An alternative path for the molecules to enter the cells using 1D nanostructures is through endocytosis. Zhao *et al.* have shown that the curvature of cell membrane around vertical nanopillar leads to an accumulation of clathrin, a protein associated with endocytosis. This effect was seen for nanopillars with diameter smaller than 200 nm [17]. These results correlate with findings when studying membrane permeability and endocytosis for human mesenchymal stem cells interfacing porous silicon nanoneedles. Also here, an accumulation of clathrin could be seen around the nanoneedles, stimulating endocytic pathways [18]. Using electron microscopy, it was also observed that the cell lipid bilayer was intact, indicating that no penetration of the cell membrane had been achieved.

1.1.3 Transfection using nanostraws

Nanotubes, as alternative to solid nanowires and nanoneedles were proposed to achieve more efficient penetrations of cells. VanDersarl *et al.* developed hollow alumina nanostraws that created a fluidic access to the cytosol, inspired by gap junction proteins in eukaryotic cells and lipid nanotubes transporting molecules between bacteria [19]. They coated polycarbonate track-etch membranes with alumina and then etched the surface to create nanostraws extruding from the membrane. HeLa cells and CHO cells were cultured on the nanostraws and molecules ranging from ions to 5000 basepair DNA plasmids could be delivered. It was observed using fluorescence microscopy that nanostraws with a diameter of 100 nm spontaneously penetrated cells cultured on top of them, enabling diffusion of small molecules into the cell from the underlying compartment. However, similar to what had been observed for NWs, nanostraws with larger diameter than 100 nm did not spontaneously penetrate the cell membrane and did therefore not lead to transfection [19].

When doing a quantitative study of the nanostraws penetrating the cell membrane, it was later found that the penetration events for 100 nm nanostraws are more rare than expected, with only approximately 7% of the nanostraws penetrating the membrane. For the CHO cells in this study, this leads to 10.7 penetrations per cells on average for a nanostraw density of $3 \times 10^7 / \text{cm}^2$ [20].

Even though transfection is possible through spontaneous penetration events occurring when using 100 nm nanostraws, there were concerns about the low transfection efficiency of molecules. In order to address this and to induce opening at all nanostraws, the same research team later introduced nanoelectroporation to the system, adding a ITO electrode plate under the device flow channel and a platinum top electrode, creating an electric field over the nanostraws [21]. By applying low voltage electric pulses to the system, local openings in the cell membrane on top of the nanostraws are achieved [22]. When transfecting CHO cells and HEK 293T cells with plasmids, the transfection efficiency was observed to be 81% and 67% respectively, while the cell viability was kept high, >95% [21]. This can be compared to 10% transfection efficiency with only nanostraws and no electroporation [19]. As opposed to solid nanostructures, where endocytosis plays an important role in the internalization of cargos, nanostraw electroporation injects cargos directly in the cytosol due to the direct opening of cell membrane on top of the nanostraws [22]. In this thesis, I use nanostraws to inject molecular beacons directly in the cytosol of clonal beta cells for investigating the possibility to measure the levels of insulin mRNA inside the cells.

Beyond morphology mediated effects, nanowires can also be integrated in electronic and optoelectronic devices. Some have been used to interface cells for manipulations and biosensing. For instance, nanowire photovoltaic core-shell

devices have been shown to stimulate neurons through the generation of a photochemical current catalyzed by Au atoms having diffused to the surface of the nanowires [23]. However, the effects of photovoltaic nanowire arrays on cells have not been explored and this is the scope of project 1 in this thesis.

1.1.4 Nanowires for biosensing

1.1.4.1 Nanowire field effect transistors

Nanowire field effect transistors (NW-FET) have been used extensively for the detection of biomolecules and cellular signals [24]. They consist of a source and a drain where current can flow in and out of the transistor, and which are connected by a NW. Adding a receptor molecule to the NW enable binding of the molecules one wants to detect. Depending on how the NW is doped, i.e. if there is an excess of hole carriers or electron carriers, binding of a polar or charged molecule to its surface leads to a change of the conductance in the NW and consequently in the device so that the presence of the bound molecules can be registered [25]. By modifying silicon NWs with biotin, picomolar concentrations of streptavidin have been detected. It was also possible to detect antibody binding in real time by modifying silicon NWs with antigens [26]. Silicon NW FETs have been successfully used for the detection of viruses. Silicon NWs coated with antibodies for influenza A showed a change in conductance for the FET when influenza A viruses were introduced to the device [27]. The ability for NW-FETs to detect biomarkers and biomolecules have since been supported by multiple studies [28], [29]. NW-FETs have also been demonstrated to record action potentials in cells. By integrating an insulating SiO₂ nanotube on top of a Si NW-FET, perpendicular to the NW, the NW gets in direct contact with the cytosol of a cell penetrated by the nanotube. If there is a change in the transmembrane potential of the cell, such as during an action potential, this change is transported in the nanotube, resulting in a detectable change in conductance in the NW and consequently in the NW-FET [30].

NWs can have other properties that can be harnessed for biosensing. One of them is their ability to act as light guiding devices, as described below.

1.1.4.2 Light guiding nanowires

Light guides are structures or devices that transport light from a light source to a different location. Light guiding is possible in structures with a refractive index pronouncedly higher than the surrounding medium. When light goes from the higher refractive index to the lower, total internal reflection occurs if the angle of the light is greater than the critical angle, allowing the light to travel within the structure.

In 2006, it was reported that ZnO NWs coated with fluorescently labeled proteins showed an increased fluorescence signal compared to control substrates, such as Si

NWs, glass, and polymer substrates [31]. The signal enhancement for fluorescently labeled molecules binding to various molecules deposited on ZnO NWs was reported in multiple studies [32]. After these findings, ZnO NWs and ZnO nanorods were increasingly used in antibody microarrays, showing comparable or lower detection limit of biomarkers compared to ELISA assays [33]. It was first thought that the increased fluorescence signal was due to NW or nanorod induced effect on the fluorophores, however, it was later shown that it was a light guiding effect with a higher and more stable fluorescence signal at the ends of the nanorods [32].

The dimensions of high aspect ratio nanostructures makes them suitable for light guiding and therefore for signal enhancement. Also for III-V NWs it has been shown that light emitted from surface bound fluorescent molecules is guided along the NW axis. For instance, this was observed for GaP NWs coated with alumina, using heavy meromyosin and fluorescently labelled actin filaments. An increased actin filament fluorescence was observed at the tip of the NW [34]. This light guiding effect has also been observed for other III-V material NWs, such as InAs and GaAs [32]. InAs NWs functionalized with different Alexa dye fluorophores through biotin-streptavidin binding have been used to study the impact of excitation wavelength on light guiding. When investigating three different excitation wavelengths (488 nm, 555 nm and 633 nm) on InAs NWs with length 4.4 μm and a diameter of 92 nm, it was observed that the fluorescence signal along the NWs varies. For the 633 nm wavelength the fluorescence signal is spread along the NW, while for the two shorter wavelengths the fluorescence signal is observed mostly at the NW tip [35]. This means that, for a given diameter, the light guiding effect is lower for longer excitation/emission wavelengths. These results are supported by a later study where GaP NWs were used to investigate the effect of NW diameter and fluorophore wavelength on light guiding. A longer wavelength showed a decreased light guiding effect, while different NW diameters was shown to be optimal for different wavelengths in respect to light guiding [36].

As mentioned above, high refraction index NWs can facilitate both focusing of incoming light and guiding of the light emitted by fluorescent molecules connected to the NW surface. NW aperture probes (NAP) based on 2-5 μm GaAs NWs indicate that a highly localized detection of fluorescent molecules can be achieved, since the probing region is less than 20 nm from the NW into the surrounding solution [37]. This results in an amplification in biomolecule fluorescence signal, enabling rare molecules to be detected. Similar amplification of fluorescence signal and improvement in signal-to-noise ratio has later been shown in light guiding GaP NWs, in combination with antibody based assays [38].

1.2 Detection of mRNA

Genes contain the information needed to fabricate all proteins in the body. When a protein is to be produced, enzymes open up the double stranded DNA and creates a complimentary copy of one of the corresponding strand. This sequence of nucleic acids is called the messenger RNA (mRNA) and the process of transferring information from the DNA to a mRNA is called transcription. After transcription, the mRNA leaves the cell nucleus and goes into the cytosol to enter a ribosome where translation takes place. In this process, the mRNA is used to make an amino acid chain, which, after folding, forms the protein.

The detection of mRNA is of interest to investigate the transcriptional state of cells. This include investigating if a cell is expressing a specific gene, in what amounts, and what factors that are involved in the regulation of the gene expression. This is of great importance for both diagnostics and in the search for disease treatments.

There are currently multiple methods to detect mRNA and oligonucleotides in solution. Some of the most popular methods are RNA microarrays, Northern blotting, Ribonuclease protection assays, in situ hybridization, quantitative PCR (qPCR), and reverse transcription polymerase chain reaction (RT-PCR).

Microarray assays can be used to detect thousands of different mRNAs at the same time. A large number of dots are printed on a microscope slide, and every dot contains a known DNA fraction or gene that will act as probes. mRNA is extracted from both the sample cells and from reference cells, such as for example cells from a patient with a specific disease and cells from a healthy patient. These two different samples are fluorescently labelled in two separate colors before they are mixed together and added to the microarray slide. The mRNA from both samples will bind to their complementary attached DNA sequence or gene (Ref Microarray Learn Science). By illuminating the microarray slide with lasers and detecting the resulting fluorescent signals, it can be visualized what genes were expressed in the two samples. The large number of mRNA that can be tested simultaneously is a benefit of the technique. However, there is a risk of false data due to degraded mRNA [39].

Another commonly used method is Northern blotting. In Northern blotting, the mRNA first needs to be extracted, often by lysing cells [40]. Agarose gel electrophoresis is then used to separate the mRNA according to size. A denaturation agent, such as formaldehyde, needs to be present during this step to avoid that mRNA self-hybridize into a secondary structure that might affect the separation [41]. The mRNA is then transferred and immobilized on a nylon membrane where it can be detected using a radioactively or fluorescently labeled hybridization probe, such as a complementary DNA (cDNA) or an oligonucleotide, that is complementary to parts of, or to the full target mRNA sequence [40]. The labeled RNA is finally visualized by being transferred to a X-ray film at -80°C , or by using

a fluorescence scanner or microscope [42]. Even though Northern blot is not the most sensitive technique, it is still one of the most commonly used techniques for detecting mRNA. It has the advantage that it is possible to get information about the size and expression levels of the mRNA. Target mRNA with a smaller size than expected can be an indication of degradation [43]. Degradation is also one of the major drawbacks of the method. There is a high risk of degradation due to RNase enzymes in all process steps. Another drawback is that relatively large amounts of mRNA is needed due to the low sensitivity.

A technique that is approximately ten times more sensitive than the Northern blot is the Ribonuclease protection assay [44]. Here, extracted RNA is mixed with a radioactively labelled antisense probe that is complementary to a section of the mRNA. This leads to a hybridization between the target mRNA and the antisense probe. When RNase is added, the hybridization protects the target mRNA section, while other non-hybridized RNA in the sample is degraded and washed away [45]. After inactivation of the RNase, the target mRNA is precipitated and can be analyzed using gel separation and autoradiography [46]. Two benefits with the Ribonuclease protection assay are its high specificity, and the fact that it is possible to measure up to 12 separate mRNA species simultaneously [47]. The drawbacks are that it is time consuming and that there is a high risk of RNase contamination [44]. It also requires a skilled operator.

Similar to the above mentioned techniques, In situ hybridization is also using the hybridization between a target mRNA and a complementary radioisotope labelled probe as a base for mRNA detection. An advantage is that it can be used for both cells and tissue [48], but at the same time the sensitivity, especially in tissue, is relatively low in conventional in situ hybridization due to high background signal and no amplification steps. There are however multiple modified techniques to increase the sensitivity, such as combining in situ hybridization with fluorescence probes, known as fluorescence in situ hybridization (FISH) [49].

When the amount of target molecules is too low to be detected, the detection method can be combined with an initial amplification step. Polymerase chain reaction (PCR) is an amplifying method where the quantitative amount of DNA is significantly increased through cycles of denaturation and annealing. When the temperature is increased, the double stranded helix splits into two single strands. The temperature is then lowered again, allowing DNA primers to attach to the ends of the target strands and creating a complementary copy of the target DNA (cDNA). The process is repeated to enable an exponential amplification of the original DNA. The same process can be used to amplify a RNA sequence. However, for the PCR process to work, a cDNA copy first needs to be generated from the mRNA. This is done using reverse transcriptase, resulting in reverse transcriptase PCR [41]. By using fluorescent dyes, the amplification process can be monitored in real time, then

named real-time PCR or quantitative PCR (qPCR). qPCR is one of the most sensitive methods for detecting mRNA. It is approximately 10 000 times more sensitive than Northern blot, it is simple to operate, but also expensive [44].

Almost all above mentioned techniques have the drawback that investigated cells have to be killed prior to measurements and therefore one only gets a snapshot of the state of the cells. One cannot see how the cells evolve over time. Moreover, since a large number of cells often is needed for using these techniques, the results only show an average of many cells, not individual cells [50]. Being able to investigate mRNA content of individual cells is valuable and can show subpopulations that are averaged in ensemble measurements. There are methods available to do single cell sequencing, however they are expensive and still require to kill the cell for analysis, preventing longitudinal studies to be performed [51]. One way to probe mRNA in individual cells without first killing the cells is to use MBs. Despite being limited to assessing a small number of genes, this method would be very useful. MBs have been used to detect mRNA in solution and in living cells. Although promising, many questions remain unanswered concerning the background signal and false positive signals [52].

1.3 My contribution

In this thesis, I contributed to the use of 1D nanotools for probing and manipulating living cells. I used photovoltaic NWs to manipulate cells. Moreover, with the aim of detecting cellular mRNA, I investigated whether using nanostraws for MB delivery would allow for a better control and understanding of the signal when detecting cytosolic mRNA. I also tested whether using light guiding nanowires could enable the detection of oligonucleotides in solution, possibly with a lower limit of detection than with current methods, which could be used to detect cellular mRNA in the future.

In the first project, “The investigation of a cell dormancy switch using photovoltaic p-i-n NWs”, I explored whether photovoltaic NWs could be used to induce cell dormancy. This project is motivated by the fact that dormancy is a very important component in cancer therapy. Cancer treatment can send cells into dormancy, and as a result, their sensitivity to the treatment is lowered [53]. One important question is whether one can develop a dormancy “switch” to further study dormancy in cells.

My second project, “Detection of *Ins1* mRNA using MBs and nanostraws”, is motivated by the currently high interest for sensing the transcriptional state of cells. Work with MBs towards this purpose has been investigated in the past. Issues have been reported, such as MBs not being delivered in the cytosol, false positive signals, and nuclear sequestration [54]. To shed light on the fate of MBs inside cells and

identify false positive signal, I have used nanostraws, which can deliver MBs in a very short time to the cytosol and monitored the signal over time in individual cells.

The third project, “Detection of oligonucleotides using MBs immobilized on light guiding NWs”, is motivated by the need of developing new and more sensitive ways of detecting mRNA. One goal is to decrease the limit of detection (LOD) for oligonucleotides, but also to decrease the experiment time consumption and cost. Here, the probing properties of MBs were combined with immobilization on light guiding NWs, to investigate the LOD of oligonucleotides complementary to the MB loop.

1.4 Outline of thesis

This thesis focus on the three projects that the attached paper I-III are based on. In chapter 2-4, the background and results for each of these projects are presented. The name of the chapter corresponds to the name of the project:

Chapter 2. Photovoltaic nanowires as dormancy switch,

Chapter 3. Detection of *Ins1* mRNA using molecular beacons and nanostraws,

Chapter 4. Detection of oligonucleotides using molecular beacons immobilized on light guiding nanowires.

Chapter 5 briefly presents the most important experimental techniques that have been used during this work.

Chapter 6 wraps up the thesis with concluding remarks and outlook.

2 Photovoltaic NWs as dormancy switch (project 1)

2.1 Background

2.1.1 Cell cycle and dormancy

The normal cell division cycle consists of the interphase and the M phase, see figure 1. During the interphase, which is the largest part of the cell division, the cell is growing in size (G_1), synthesizing genetic material (S), and prepares for division by growing further and producing new building material needed in the daughter cells (G_2) [55]. The M phase consists of mitosis and cytokinesis. During the mitosis, the nuclear DNA is divided, and the cytosol can then split into two and form daughter cells during the cytokinesis phase [56]. In addition to this cell division cycle, the cell can enter a dormant G_0 phase, where the cell retains its normal tasks, but do not undergo cell division [57]. Different cell types spend different amount of time in the G_0 state. Neurons and other cells that divide very seldom or not at all spend most of their life time in the G_0 state, while for example cancer cells or epithelial cells lining the inside of the intestines, divide frequently and spend much less time in the G_0 state [57].

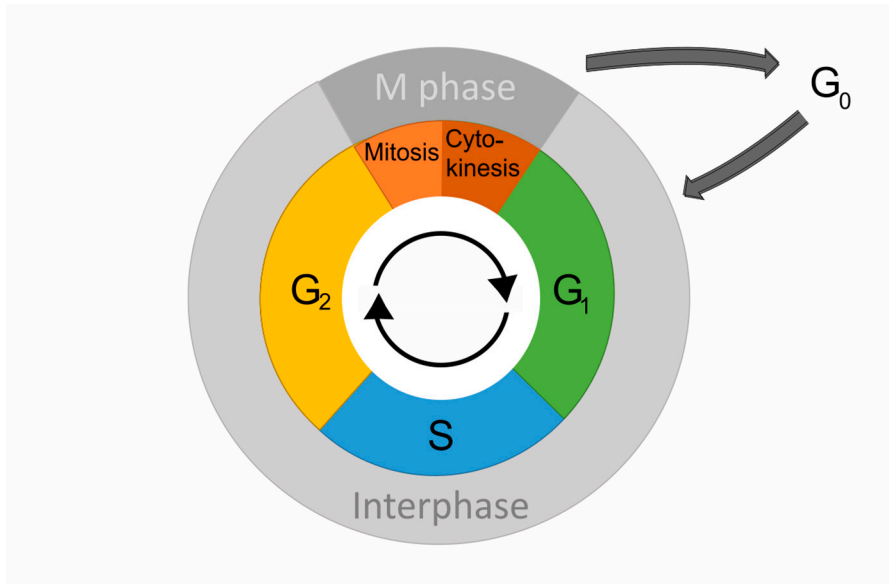


Figure 1. The cell cycle including cell division and dormant G_0 phase. During the G_1 , S, and G_2 phases, the cell prepares for cell division. Splitting of the DNA takes place during the mitosis, and the cytosol finally split into two during the cytokinesis phase.

Many chemotherapeutical treatments act by damaging mechanisms in some parts of the cell division. It then becomes an issue when cancer cells are in a dormant state, avoiding the treatment aimed to kill them, leading to it being difficult to achieve efficient chemotherapy [58], [59].

Dormant cancer cells leading to reoccurring cancer in the form of metastases is a large reason for most cancer death cases [60]. A need for targeting dormant cancer cells has been identified to improve chemotherapeutic efficiency and minimize adverse effects of therapeutic drugs. Different methods, such as using nanoparticles for more efficient drug delivery have shown promising results [61]. A cell dormancy switch would make it possible to send cancer cells into dormant state in a controlled way, while studying the effect of therapeutic compounds in vitro. Consequently, we could get an increased knowledge in the dormancy phenomenon and potentially have a tool useful in cancer research. As demonstrated in paper I, photovoltaic NWs can be used as such a switch.

2.1.2 Function of photovoltaic NWs

Semiconducting NWs are nanostructures with a high aspect ratio, and can therefore be referred to as one-dimensional. They have a diameter of approximately 10 nm to 100 nm, while the length can be several micrometers [62]. The high aspect ratio also

give the NWs specific properties, and by combining different semiconducting materials, these properties are of interest in applications such as transistors [63], solar cells [64] and light emitting diodes (LED) [65]. If a NW, or parts of a NW, is composed of only a single material, it is considered to be intrinsic, i.e. without addition of impurities.

Semiconductor materials can be doped with impurities, resulting in extra electrons or vacancies (holes). A p-n junction is the interface between two doped semiconductors, where the n-doped section contains extra electrons, and the p-doped section contains extra holes. When making devices such as transistors, solar cells, and LED lights, the p-n junction is very important [66]. At the interface between the doped materials, a depletion region is formed. Free electrons from the n-doped side and holes from the p-doped side can here diffuse and recombine [67]. In figure 2, a schematic of a p-n junction is illustrated. The probability for an electron/hole pair to be dissociated, and thereby creating a current, is increased by increasing the width of the depletion region. The NW will then have a p-i-n junction with an intrinsic section.

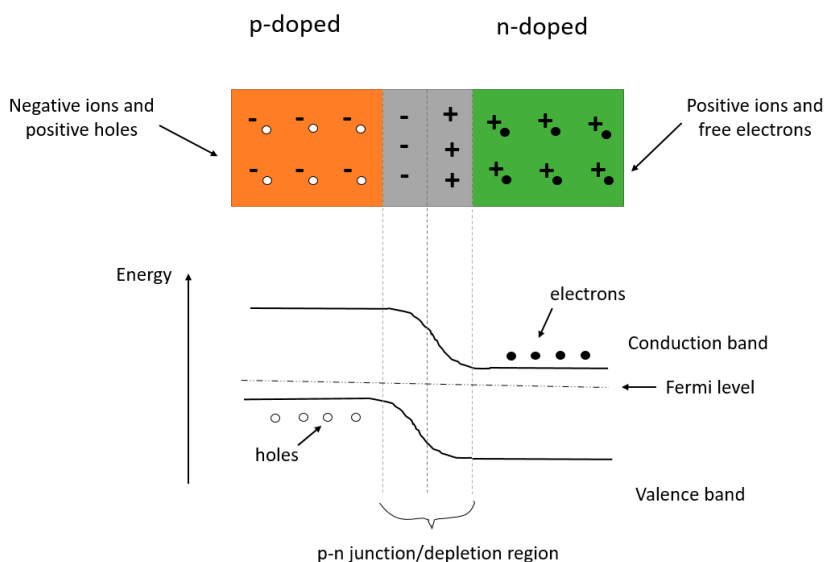


Figure 2. Schematic of a p-n junction. At the interface between the two doped semiconducting materials, electrons and holes can diffuse and recombine. This creates a depletion region and an electric field. The lower part of the figure shows the p-n junction energy band diagram.

In the case of photovoltaic NWs used in solar cells, the junction is connected to create a closed circuit. Incoming light is then absorbed by the NWs if the energy is greater than the band gap. This will cause an electron to excite up to the conduction

band, leaving behind a hole in the valence band. This way, an electron hole pair is created in the p-i-n junction and these carriers will move in the structure due to the created electric field, causing a current to run in the circuit [68].

In addition to optoelectronic properties, NWs have been shown to be a good culture substrate for cells [69], [70]. Biocompatibility studies have shown that cells are not harmed by NW substrates, which is a prerequisite for using NW substrates for interacting with cells. Many studies investigating the interactions between cells and NWs are focused on the effects of NW topography [71]–[74]. However, there is less data available about a possible effect of the optoelectronic properties of the NW on the cells.

In the case of photovoltaic NWs, one question was whether the photovoltaic properties of the NWs could affect the cells, in addition to a potential topographical effect. In my project 1, I tried to answer this question by seeding cancer cells on photovoltaic NWs and exposing them to light illumination. I then studied the proliferation of the cells.

2.2 Results

2.2.1 Characterization of the NWs

The Au particles used to facilitate the NW growth had a pitch of 500 nm and were seeded in a hexagonal pattern. The resulting InP NWs had a length of $2.8 \pm 0.2 \mu\text{m}$. Figure 3 shows a SEM image of the NW pattern.

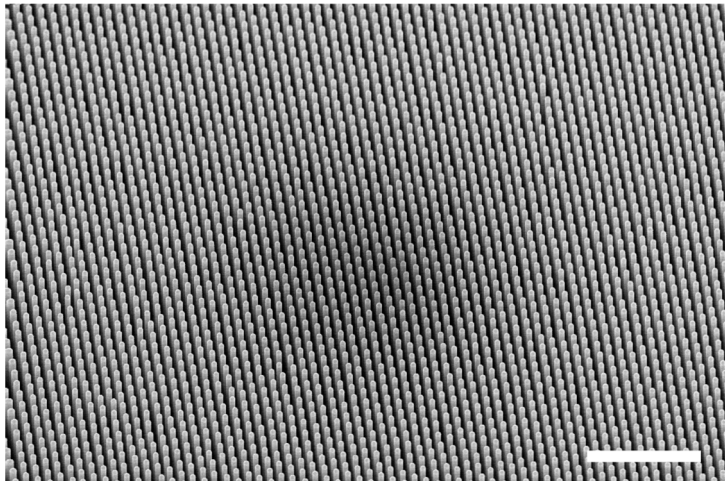


Figure 3. SEM image of the InP NW array used in the dormancy switch project. Scale bar 5 μm .

EBIC was performed by Lukas Hrachowina at division of Solid State Physics, Lund University, to investigate the electrical properties of the p-i-n junction of the grown NWs. Figure 4a shows a SEM image with a cross section of the NW array, where one NW has been false colored to show the proportions of the p-doped, intrinsic, and n-doped parts. As the NW is exposed to the electron beam in a SEM, a current will be induced in the NW, shown by the red EBIC curve in figure 4b.

When the electron beam hits parts located far away from the p-i-n junction in the NW, no current is induced since the electric field here is too low. Within the p-i-n junction, the electric field creates a driving force on the electrons and holes created from an electron-hole pair, and a current is measured. The intrinsic section of the p-i-n NW is in fact slightly p-doped to even out extra electrons in our case. This leads to a maximum electric field at the interface of the n-doped section and the intrinsic section. As can be seen in figure 4b, the measured current is in fact at its highest value in the interface between the n-doped region and the intrinsic region. The current is then stable along the intrinsic section and drops as we enter the p-typed section. All together, these results shows that the p-i-n junction acts as expected.

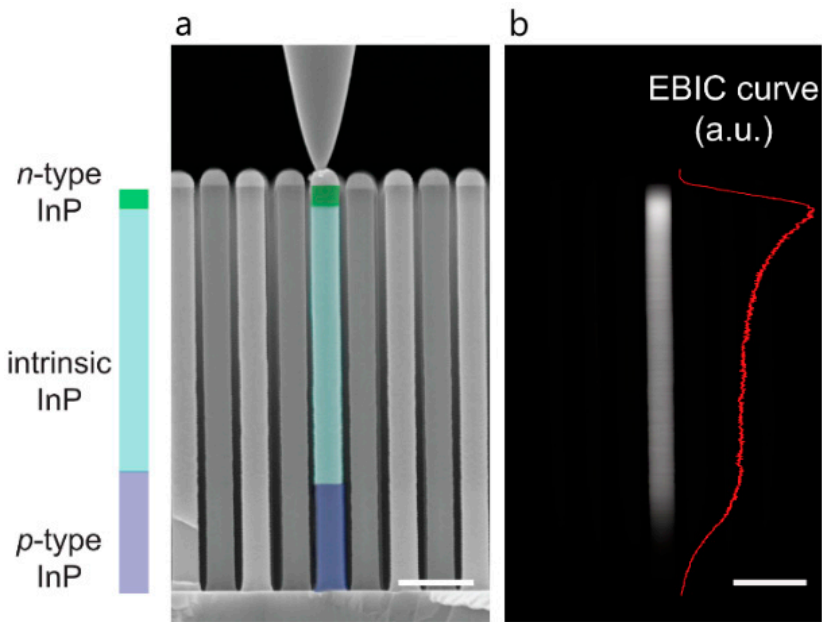


Figure 4. Characterization of the InP NWs used in the dormancy switch project. (a) SEM image with false colored NWs cross section during EBIC. (b) EBIC curve of the p-i-n NW. Scale bars in (a) and (b) is 500 nm.

2.2.2 Effect of illumination on cells seeded on p-i-n NWs

Illumination experiments were performed to investigate the proliferation of cells seeded on photovoltaic NWs. Figure 5 shows a SEM image of one A549 cell seeded on the InP NWs.

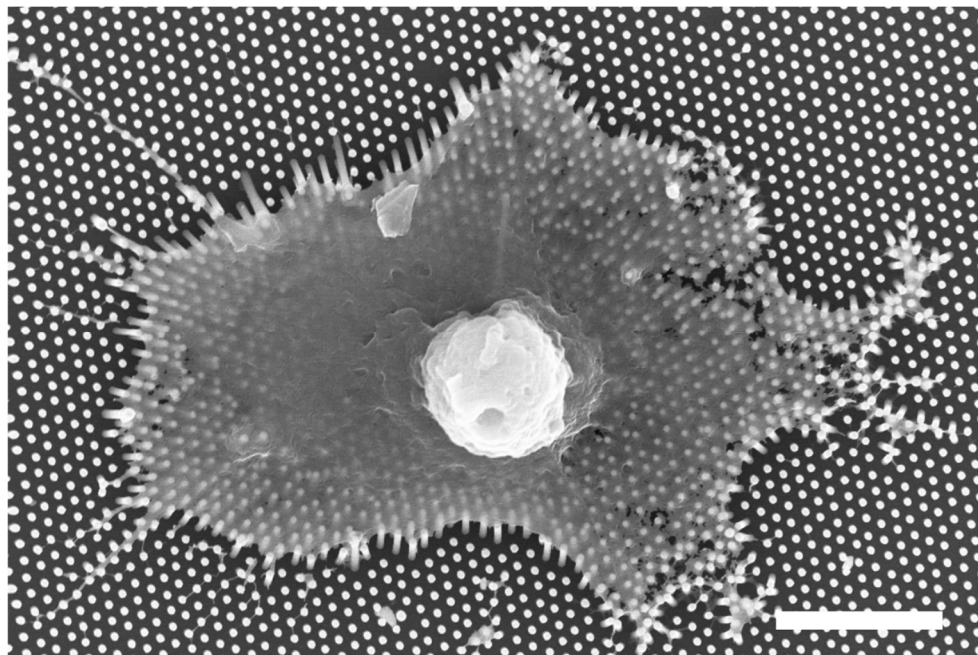


Figure 5. SEM image of a A549 cell seeded on the InP NW array

Cells and NWs were cultured in dark or light conditions for 48 hours after seeding and were then labeled with anti-Ki67 and secondary antibodies to visualize the amount of Ki67 positive cells. Ki67 positive cells represent cells in an active cell cycle phase, i.e. not in the G_0 phase. The results can be seen in figure 6. When comparing cells seeded on photovoltaic NWs, the percentage of cells in active states (Ki67 positive cells) was significantly higher for cells cultured in the dark compared to the cells cultured under light conditions.

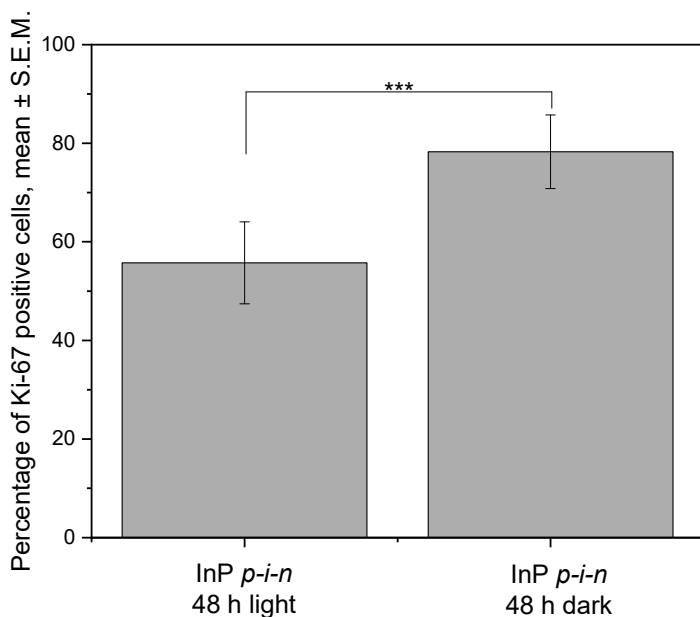


Figure 6. Bar graph showing the percentage of Ki67 positive cells among cells seeded on InP *p-i-n* NWs and kept 48 hours in dark or light conditions. Significance level in one-way ANOVA ***: $p \leq 0.001$.

The results in figure 6 shows that there is an effect on the cell proliferation when cells are exposed to the combination *p-i-n* NW substrate and light. One possible explanation for this could be that the activated NWs harm the cells, sending them into apoptosis. To investigate whether the non-active cells were dormant or dying, TUNEL labeling was performed. TUNEL binds to one end of degraded DNA which is a sign of apoptotic cells. The results from TUNEL labeling showed that the cells are not apoptotic to any large extent. This suggests that the decreased amount of Ki67 positive cells for cells in light conditions in figure 6 instead arises from an increased proportion of dormant cells.

Inactive InP NWs (InP *i*) and glass substrates were used as a control to make sure any difference in cell behavior does not origin from the light exposure itself, see figure 7. There is no significant difference in the proportion of Ki67 positive cells between cells seeded on glass and inactive NWs in dark or light conditions, which confirms that the lower proportion of proliferative cells is not due to phototoxicity.

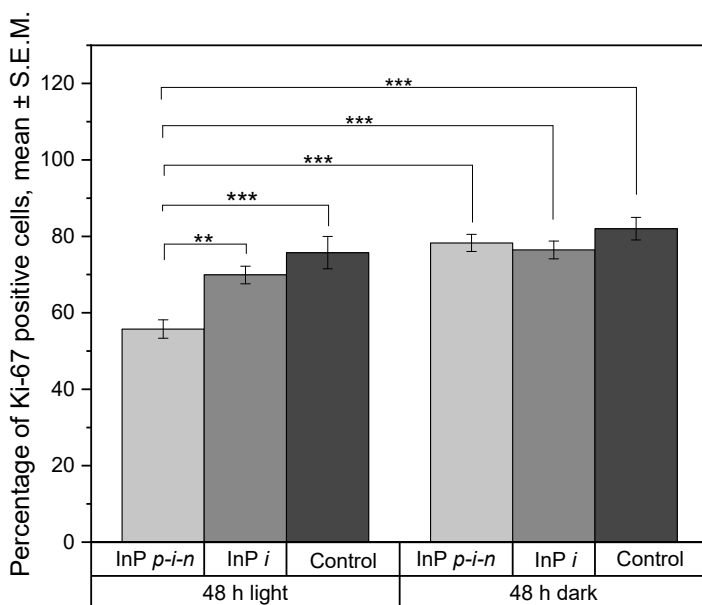


Figure 7. Bar graph showing the percentage of Ki67 positive cells among cells seeded on InP *p-i-n* NWs, inactive (*i*) InP NWs, and glass controls. The cells were cultured for 48 hours in dark or light conditions. Significance level in one-way ANOVA ***: $p \leq 0.001$, ** $p \leq 0.01$.

The fact that there is no difference in the proportion of Ki67 positive cells in cells seeded on glass, inactive NWs and *p-i-n* NW in dark conditions supports the fact that the lower proliferation on illuminated *p-i-n* NW is not due to the NW topography. The fact that there is no significant difference between inactive NWs in dark and light regarding the proportion of Ki67 positive cells supports the fact that the differences observed in the *p-i-n* in light is also not due to phototoxicity, but to the photovoltaic properties of the NWs. As the light is absorbed by the *p-i-n* NW, an electron-hole pair is created in the *p-i-n* junction, giving rise to a current into the surrounding medium at the *n*-doped section of the NW.

Another control experiment was performed to investigate if the photovoltaic property that affected the cells was involving current or voltage build-up. Both photovoltaic and inactive NWs were coated with a 10-15 nm thin layer of SiO₂ using ALD. These substrates were then used in the same experiments as for non-coated NWs, i.e. cells were seeded on them and were cultured for 48 hours in light or dark conditions. The cells were then labeled and the amount of Ki67 positive cells were counted.

By adding SiO₂ coating, which is a dielectric material, the connection between the photovoltaic NW and the surrounding medium is opened. Therefore, the current is

replaced by a voltage build up in the NWs. With the SiO₂ coating, no significant difference can be seen regarding Ki67 positive cells, see figure 8. This shows that charge injection is key for sending the cells into dormancy. Any effect of the voltage built up on the cell proliferation could not be seen.

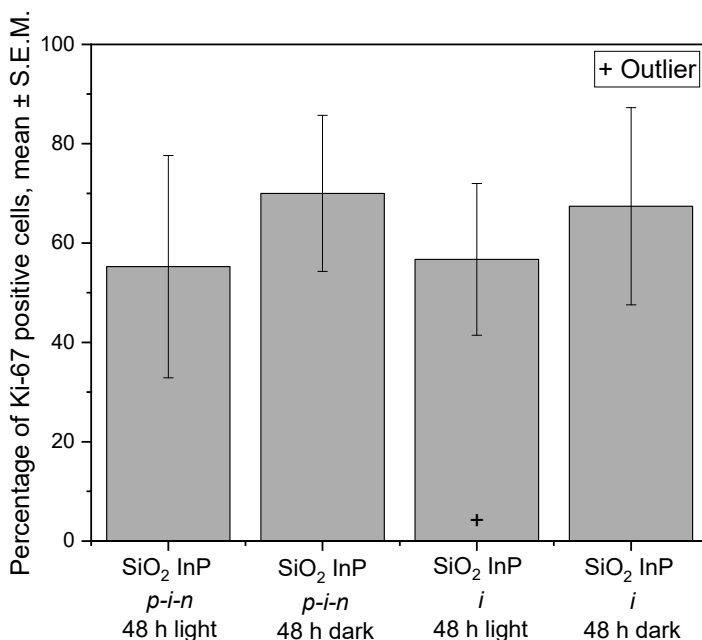


Figure 8. Bar graph showing the percentage of Ki67 positive cells seeded on SiO₂ coated InP *p-i-n* and inactive NWs. No statistically significant difference between the samples could be observed for *one-way ANOVA* *: $p < 0.05$.

In order to investigate whether the cell population recovers after treatment (i.e. whether dormancy is reversible), cells were left in the dark for 48 hours after the initial 48 hours of dark or light conditions. The results, that can be seen in figure 9, show that the number of Ki-67 positive cells increases from 55 to 67%, showing that the cell population recovers (at least partly).

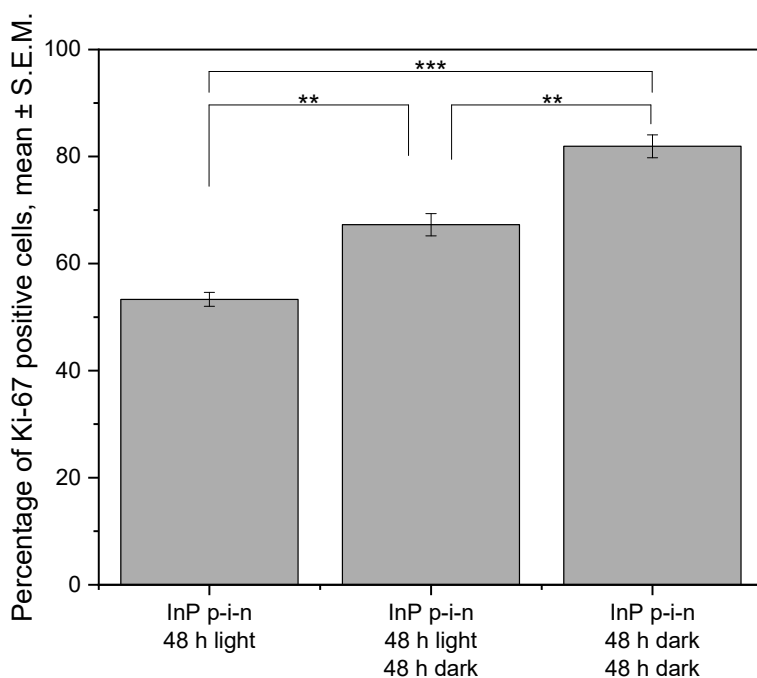


Figure 9. Bar graph showing the percentage of Ki67 positive cells seeded on p-i-n InP NWs. After the cells had been exposed to light or dark conditions for 48 hours, they were left in dark to recover for another 48 hours.

From the results illustrated in figure 6 and figure 7, one can draw the conclusion that light illumination induces cell dormancy in cells seeded on photovoltaic InP NWs. The low percentage of TUNEL positive cells (1-4%) indicates that the cells are not dying to any large extent, instead suggesting that the cells actually are in dormant state. The fact that no significant difference in amount of Ki67 positive cells could be seen for active and inactive NWs coated with SiO₂, indicates that it is current and not voltage that is causing the difference for non-coated NWs. The difference between the amount of Ki67 positive cells after dark and light conditions was decreased when the cells were put back in dark conditions for recovery. This shows that the cell population recovers to some extent.

3 Detection of *Ins1* mRNA using MBs and nanostraws (project 2)

3.1 Background

3.1.1 mRNA detection in cells

If one can quantify a specific mRNA in the cytosol, one can sense the transcriptional state of the cell, which is a reflection of the gene expression level for that specific sequence/protein. A benefit with current techniques such as microarrays and qPCR for sensing cellular transcriptional states, is that they can give results with high sensitivity on all genes [54]. However, there are also several drawbacks associated with these methods. One drawback is that the investigated cells have to be killed prior to measurements and therefore one only gets a snapshot of the state of the cells. One cannot see how the cells evolve over time. Moreover, since a large number of cells is needed for using these techniques, the results only show an average of many cells, not individual cells [50]. There are methods available to do single cell sequencing, however they are expensive and still require to kill the cell for analysis, preventing longitudinal studies to be performed [51]. One way to probe mRNA without first killing the cells is to use MBs.

3.1.2 Structure and function of MBs

MBs are oligonucleotide probes designed to complement a specific nucleic acid sequence, and can thereby be used to detect these sequences in an extracellular or intracellular environment [75]. The MBs has a hairpin structure built up by a stem and a loop. By connecting a dye molecule to one end of the MB and a quencher to the other end, as can be seen in figure 10, the MB can be used to detect specific nucleic acid sequences using fluorescence [76]. As long as the MB is closed, the distance between the dye and quencher is short and the dye signal is suppressed by the quencher. When the sequence in the loop gets in contact with a complementary nucleic acid sequence, they hybridize, causing the stem to break open and the ends of the hairpin to go apart [77]. The distance between the dye and the quencher is then increased, causing the dye to light up [78].

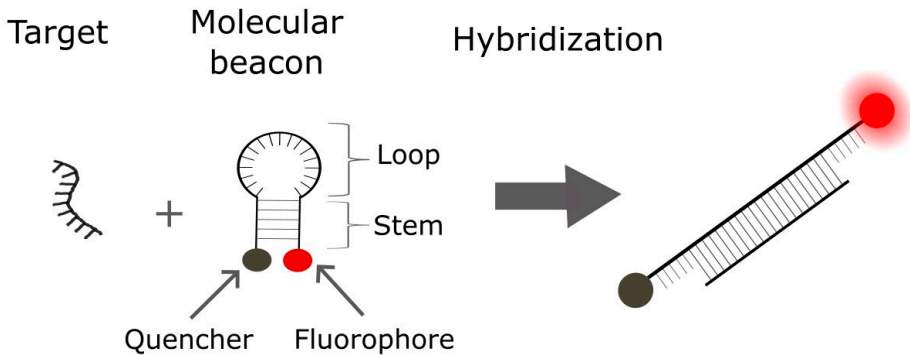


Figure 10. Structure and function of MBs. The MB will unfold when the probing loop hybridizes with a complementary target nucleic acid sequence. As a result, the distance between the fluorophore and quencher increases and the fluorophore lights up.

Apart from detecting the presence of a specific nucleic acid sequence, MBs also possibly make it possible to probe concentrations of the chosen target, by measuring the intensity of the MB fluorescence [79]. This can be used in cells to report the presence of a specific mRNA and its variation in concentration as a function of time.

One limitation of using MBs is that one can only use a limited number of probes at the same time, around one to four. This is due to the fact that the excitation and emission wavelengths of the fluorophores should not overlap for the different probes, resulting in a limited number of colors that can be used in the imaging. Even though this limitation could be a clear drawback for the system, it is overshadowed by the possibility of making longitudinal measurements over many cells at the individual cell level.

3.1.3 Challenges when designing suitable MBs

There are a number of challenges to keep in mind when designing MBs. The target nucleic acid sequence in cells (mRNA) is usually thousands of base pairs long. Within that sequence, one needs to select a sequence of around 15-30 base pairs that the MB will hybridize to [80]. The chosen sequence has to be unique for the target sequence in order to avoid hybridization with other unwanted mRNA targets. It should also be a section of the mRNA target that is not self-hybridized, so that it is open and accessible for the MBs [81].

One also has to consider the hybridizing strength for the MB stem, which needs to be high enough to ensure a closed state in the absence of target mRNA, but not to the extent that they will not open upon MB hybridization with its complementary

sequence. The stem of the MB should preferably be approximately 5 base pairs long [76].

Depending on the nucleic acids within the sequence, MBs can fold and self-hybridize in different ways. It is important that the open loop is large enough to enable the stem to open upon hybridization with its complement sequence [82].

3.1.4 MBs in cells

MBs have been shown to be a good tool to visualize mRNA hybridization and distribution in cells [83], [84]. Different modifications and linkers to the MBs are explored to increase signal to noise and to find new applications. MBs designed as 2'-O-methyl oligonucleotide probes have been suggested to better avoid degradation inside of cells [84]. MBs with attached nanoparticles can be used both for mRNA detection and as a part of the therapeutic treatment of cancer [85]. Modifications, such as adding phosphorothioate (PS) linkages can increase the stability of the MBs, but at the same time increase the risk of unspecific binding if the proportion of the PS is not optimized [86].

The use of MBs is promising to overcome the need of killing cells and using large quantities of cells for the analysis. There are however several difficulties to think about regarding MB design and delivery when using them for sensing the transcriptional states of cells. Apart from the challenges already mentioned in the previous section regarding the MB design, one also needs to consider the intracellular environment. The MBs have been shown to work very well outside the cellular environment. When they get inside the cell, things get more complicated [82].

There have been indications that MBs upon entering the cell, rapidly relocate to the nucleus and then have a decreased chance to meet and hybridize with its target mRNA. Studies have been made where the MBs are linked to streptavidin to slow this movement down, increasing the chance of hybridization [87]. However, if an excess of streptavidin would be present, there is a risk of these interacting with biotin on the cell surface and interfering with normal cellular behavior. To some degree, this adverse effect can be minimized by purification of the MB-streptavidin complex, where excess streptavidin is removed prior to measurements.

To reflect the amount of a given mRNA, the MBs need to be located in the cytosol. However, when delivered using lipid nanoparticles, which is the standard way to deliver MBs to cells, they enter cells through endocytosis and tend to end up in cellular compartments, such as lysosomes [88]. In this case, they will not be in contact with the cell mRNA. Multiple studies have been made to try to overcome the difficulties of MB delivery [89], [90]. One possible solution to get the MBs into the cytosol could be the use of microinjections [91]–[93]. However, microinjection

means injecting one cell at the time, which is not scalable. An alternative is to inject the MBs using nanostraws, which is done here, in project 2.

3.1.5 Nanostraws for intracellular delivery

Nanostraws are hollow alumina nanotubes that, in general, have a diameter of 100-200 nm and that are 1-3 μm long [94]. The nanostraws, working as a nanoinjection tool, allow the MBs to reach the cytosol of living cells, and open up for repeated injections while monitoring individual living cells over time, which would be a great improvement over current methods. Moreover, due to the structure of the nanostraw substrates, a large number of cells can be injected at the same time. Different molecules have successfully been injected in cells using nanostraws in the past, such as Propidium iodide, RNA and DNA plasmids [21], [95], [96]. Nanostraws can also be used to extract cellular content for measurements of intracellular mRNA [97].

By combining nanostraws with low voltage pulses of nanoelectroporation, nanoscale pores open in the cell membrane, resulting in less stress for the cell than during standard electroporation [22]. This way, intracellular delivery is facilitated and the viability of the cells is kept high. In project 2, we combine the probing benefits of MBs with the intracellular delivery of nanostraws. The cells used were INS-1 beta cells seeded on nanostraws, and the MBs were designed to probe for *Ins1* insulin precursor mRNA.

3.2 Results

3.2.1 Functionality of MBs

The designed MBs had the sequence ATTO647N-[CCT GC T TGC TGA TGG TCT ATG ATT G]CA GG-IAbRQ, where the sequence within brackets are complementary to nucleotide 20 to 44 of the insulin precursor *Ins1* mRNA in INS-1 beta cells. The letters in *italic* indicate the nucleotides that forms the MB stem, the bold letters the MB loop, ATTO647N is the fluorescence dye, and IAbRQ (Iowa black RQ) is the quencher.

To test the functionality of the designed MBs, they were introduced to a complementary oligonucleotide sequence and the fluorescence signal was measured using a fluorescence plate reader. When the complementary oligonucleotides were present, the fluorescent MB signal clearly increased compared to when MBs were on their own, see figure 11. This tells us that the MBs are functional and hybridize as expected with their targets. When DNase is added to the MBs, the MBs degrade and fluorescence increase due to loss of proximity between the fluorophore and the

quencher. A 2'-O-methylated version of the MB and a MB modified with PS were also run in identical measurements, but without any conclusive behaviour (data not shown).

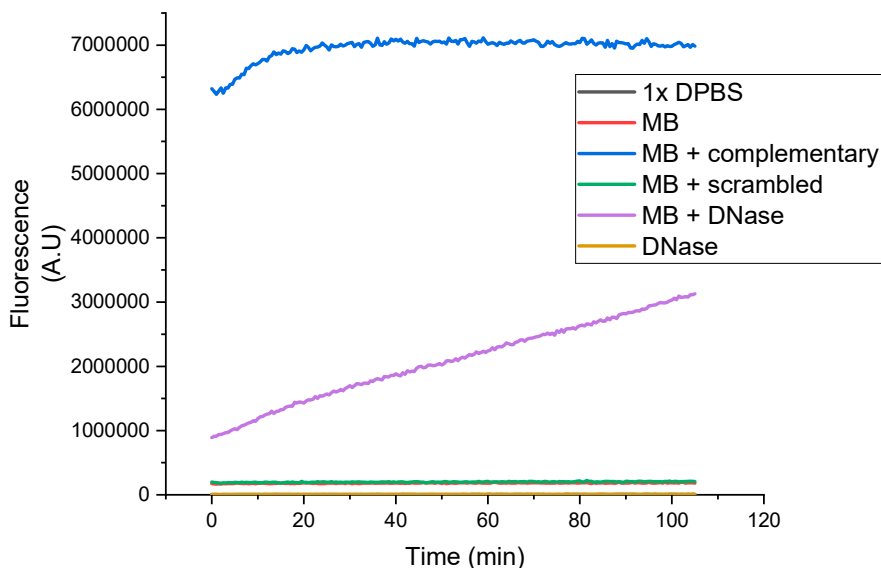


Figure 11. Fluorescence signal of MBs over time. MBs were combined with either complementary oligonucleotides, scrambled control nucleotides, or DNase. Hybridization between the MBs and the complementary oligonucleotides lead to an increase in fluorescence, while DNase degrade the MBs. Upon degradation, the fluorophore and quencher are released and then no longer in close proximity with each other, resulting in the fluorophore lighting up.

3.2.2 Cell viability after intracellular delivery of MBs

After the MBs had been shown to act as expected outside the cytosol, they could be injected into cells. INS-1 beta cells were seeded on nanostraws and nanoelectroporation was used to inject the MBs. To investigate the effect of MB injection on cell viability, cells were removed from the nanostraws after 1h and 24h, briefly incubated with DAPI, and run through a flow cytometer. As control, INS-1 beta cells were seeded on nanostraws and then injected using nanoelectroporation, but without MB cargo. It was observed that the proportion of live cells after MB delivery did not change significantly after 1h and 24h compared to the control, as can be seen in figure 12. However, one also needs to take into consideration the fact that cells that had died on the nanostraws will be removed already during the washing steps prior to flow cytometry. This means that the percentage of cells alive in these measurements may be misleading. Instead, one also needs to look at the cell concentration of the samples analysed using flow cytometry at the given time points. At 24h after MB delivery, the cell density has decreased slightly compared to the

control, which indicates that there could be some cytotoxicity associated to the injection of MBs during this time period.

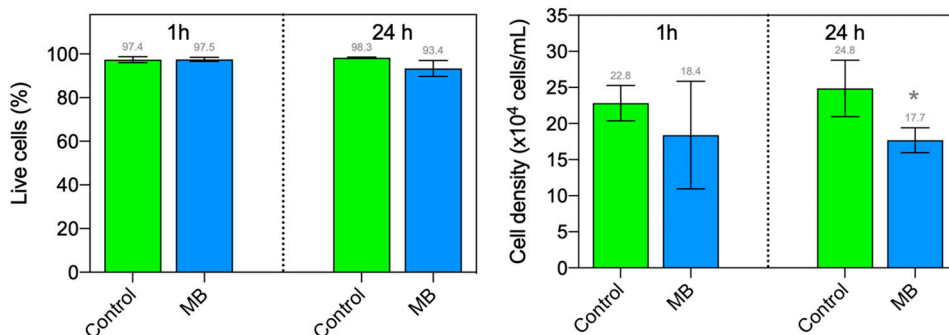


Figure 12. Cell viability 1h and 24h after MB delivery. Left plot shows the percentage of cells alive for the 2 time points, comparing with control. Right plot shows the cell density at the same time points. Two-way ANOVA, *:p=0.039

3.2.3 Monitoring insulin mRNA using *InsI* MBs

One of the goals when choosing the *InsI* mRNA was to investigate if the MBs could monitor the production of insulin precursor *InsI* mRNA over time. To do this, cells were cultured with glucose free medium for 3 hours before the *InsI* MBs were injected using the nanostraws and nanoelectroporation. Some of the cells then were placed in new, high glucose medium, while control cells were still kept in a glucose free environment. The cells were imaged using fluorescence microscopy 1, 5, 10, 15, 30 and 45 minutes after MB delivery. Since the hybridization between *InsI* MBs and the *InsI* mRNA is taking place in the cytosol, the fluorescence signal from cell cytosols was measured (the nucleus signal was excluded). The fold change $\alpha(t)$ of the cytosol fluorescence upon glucose stimulation was calculated as:

$$\alpha(t) = \frac{\left[\frac{I_c(t) - I_{bg}(t)}{I_c(1 \text{ min}) - I_{bg}(1 \text{ min})} \right]_{Stim}}{\left[\frac{I_c(t) - I_{bg}(t)}{I_c(1 \text{ min}) - I_{bg}(1 \text{ min})} \right]_{Control}}$$

Where $I_c(t)$ is the intensity in a small square in the cytosol at time t , $I_{bg}(t)$ is the background intensity at the same time point, $I_c(1 \text{ min})$ is the intensity 1 min after MB injection, and $I_{bg}(1 \text{ min})$ is the background intensity 1 minute after MB injection. Stim and Control indicates cases where cells are exposed to high glucose and no glucose medium, respectively.

For cells exposed to high glucose medium, the fold change of the MB signal from the cytosol increased approximately 2.5 times after 45 min, see figure 13. This supports previous studies where the increase of MB fluorescence signal in the cytosol is not increasing more than 2.5 fold compared to the background, despite a high concentration of target mRNA in the cell [87]. The hypothesis is that most MBs rapidly enter the nucleus instead of hybridizing with their target mRNA in the cytosol.

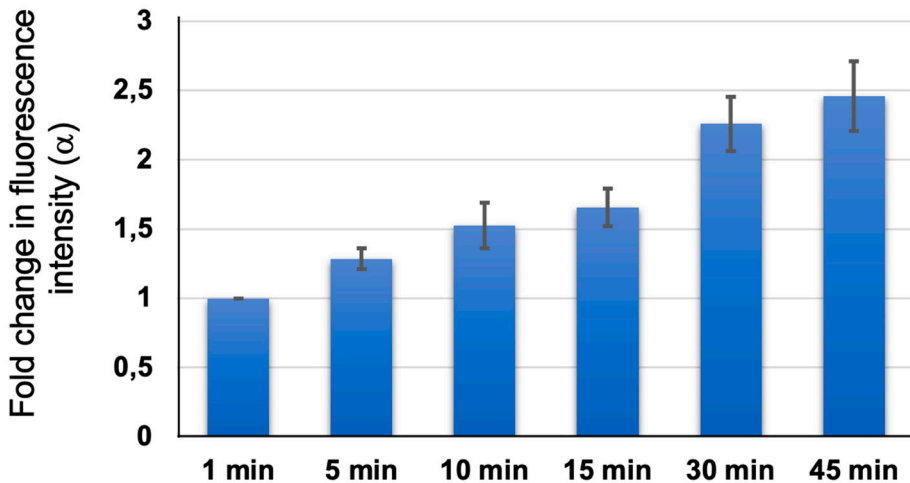


Figure 13. Fold change fluorescence intensity for MBs in cytosol at different time points after MB injection.

3.2.4 Fate of *Ins1* MBs in cells in time and space

When imaging the cells approximately 2 hours after MB delivery, fluorescence with a punctuated appearance was observed in the cytosol. Only to some degree this MB signal colocalized with DNA stain when the cells were stained with Hoechst dye. We speculate that this could be due to MB degradation or a DNA signal too weak to observe. The cells were then instead stained with lysosome marker LysoTracker and mitochondria marker Mitotracker 24 hours after MB delivery, to investigate the fate of the MBs. The MBs colocalized with mitochondria but only partly with lysosomes, see figure 14.

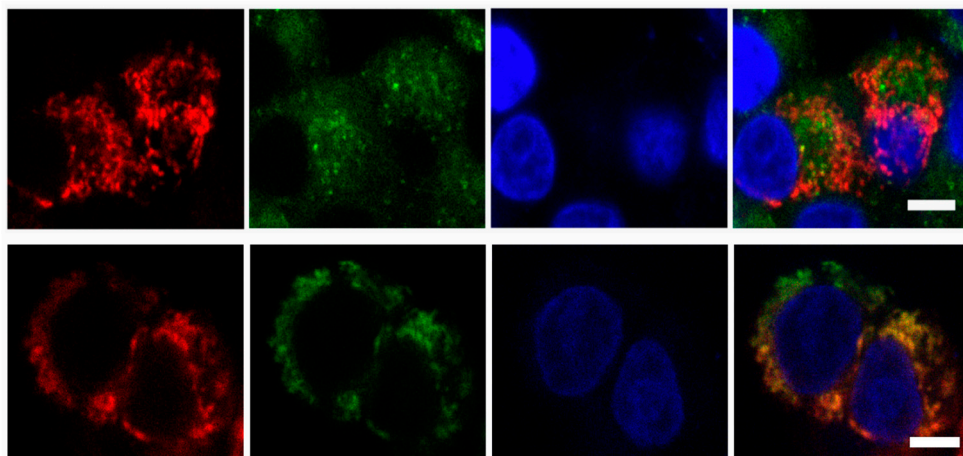


Figure 14. MBs fluorescence in beta cells when counterstained with Lysotracker (top panel) and Mitotracker (bottom panel). Red color shows MB fluorescence signal, blue is DNA (Hoechst), and green is lysosome (top) and mitochondria (bottom) signal. Right panels: composite images.

A previous study showed a punctuated appearance for MBs fluorescence colocalizing with mitochondria (which are negatively charged) if the dye of the MB was positively charged, but not if the fluorescent dye was negatively charged [84]. Even though DNA is negatively charged, the authors suggested that the charge of the dye would cause an accumulation of the MBs at the mitochondria, assuming the dye is still attached to the DNA part of the MB. Based on the fact that we can not see any colocalization between MB and DNA 24 hours after MB injection, we instead speculate that the MBs have been degraded, and the positive dye can then alone accumulate at the mitochondria.

3.2.5 Scrambled MBs as control for specificity

To make sure that the results above were not due to unspecific binding and MB degradation, a MB with scrambled sequence loop was used as a control. This was injected the same way as the *Ins1* MB, and the fluorescence was observed over time. Interestingly, the fluorescence signal of the nucleus increased strongly already 1 minute after MB injection for the scrambled MBs, and then showed a punctuated appearance in the cytosol faster than the *Ins1* MB, see figure 15.

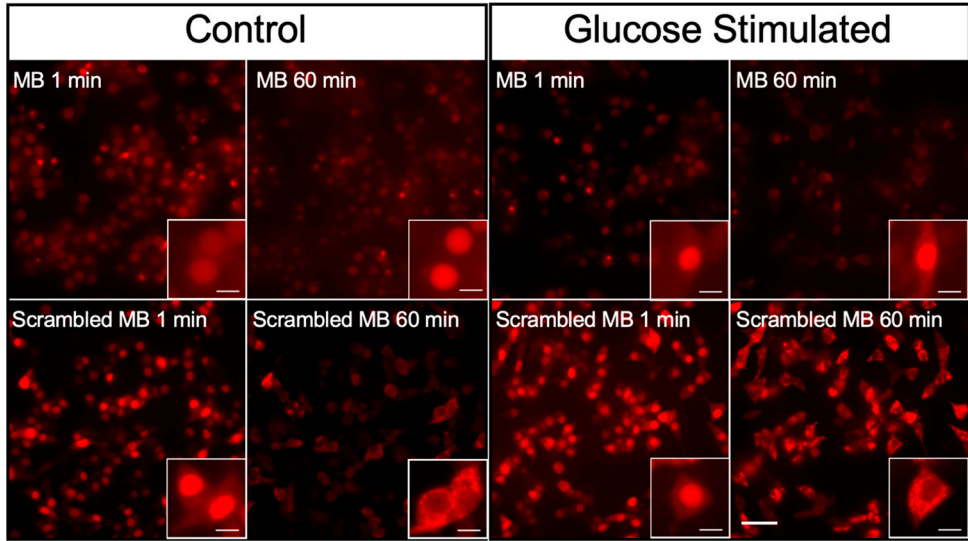


Figure 15. Fluorescence signal from MBs complementary to *Ins1* mRNA and MBs with scrambled sequence. Images captured 1 min and 60 min after MB injection, for both glucose stimulated cells and control cells.

A hypothesis is that the scrambled MBs take the same path as the real *Ins1* MBs, but since they are not hindered by hybridization in the cytosol, they are transferred to the nucleus faster. Then MB degradation takes place on the way to or from the nucleus, leading to free fluorescent dye with positive charge that can accumulate at the mitochondria and creating a punctuated appearance. For scrambled MBs, glucose stimulation accelerates this process. We speculate that this is an indication that the degradation is ATP dependent.

Nanostraws in combination with nanoelectroporation was here shown to be an efficient way of injecting MBs into INS-1 beta cells. After injection, both *Ins1* MBs and scrambled MBs rapidly move to the nucleus, before reentering the cytosol and creating a punctuated appearance. This process is faster for scrambled MBs than for *Ins1* MB, and it is speculated that this is due to the scrambled MB not being hindered by hybridization in the cytosol. The fluorescence signal in the nucleus could most probably be considered as false signal due to MB degradation rather than oligonucleotide hybridization. This is supported by the fact that the transport of scrambled MB is accelerated by glucose stimulation. This indicates that an ATP dependent process is involved, such as enzymatic degradation. The punctuated appearance of the MBs in the cytosol colocalize with mitochondria, but not so much with lysosomes. It is speculated that the positive dye of the MB, accumulate at the negatively charged mitochondria after MB degradation. The fluorophore is then a free molecule without a negatively charged strand of DNA attached to it.

Our results suggest that MBs can indeed hybridize with and detect oligonucleotides when in a controlled in vitro environment, but when MBs are injected into cells, most of them are rapidly degraded, resulting in false positives. This means that the original intention to probe for *Ins1* mRNA could only be partly achieved. The MBs were successfully injected to the cells, using nanostraws and nanoelectroporation. Some fraction of the MBs also did hybridize with its mRNA, considering the increase in fold change. But overall, injecting MBs into cells is suggested to be a misleading way to probe for mRNA.

4 Detection of oligonucleotides using MBs immobilized on light guiding NWs (project 3)

4.1 Background

4.1.1 Immobilization of MBs

Detection of biomolecules in different kinds of sensing applications is important for the development of faster, cheaper, and more sensitive probing devices, such as screening tests for disease detection. As been described in a previous chapter, MBs are single stranded DNA sequences in a hairpin configuration. They are a useful tool for probing biomolecules in cells. In addition to injecting MBs into cells, as was done in project 2, the MBs can be immobilized on a surface for detection of biomolecules in a solution. Different immobilization methods and substrates have been suggested in the past. Some examples of substrates used are: PMMA [98], photonic bandgap structures [99], and metal surfaces [100]. These techniques all have different limit of detection (LOD) and setup complexity. Studies have also shown that paper-based lateral flow strips could be a promising option when developing a probing method that is cheap and easy to use [101]. There is however still a need for developing more time efficient techniques for sensing biomolecules with high sensitivity.

4.1.2 Limit of detection (LOD)

When detecting biomolecules using MB immobilized on a substrate, different LODs have been reported, ranging from several micromolar for detection on metal surfaces [100], down to sub femtomolar scale for lateral flow strips [101]. Apart from the naked MB signal, there are ways to amplify the fluorescence signal. This can be done either before or during measurements. A common strategy is to amplify the target using qPCR before doing the fluorescence detection measurements. This way, the need for high sensitivity is lower, since the target concentration is increased to a detectable level. Drawbacks of this method is however that it is often costly and

time consuming [102]. Another strategy is to use enzymatic cleavage during the fluorescence measurements. One target can then induce cleavage of multiple MBs, resulting in an amplification of the fluorescence signal. Although one can get LOD on the order of femtomolar with this method, the risk of false signal is high, since unspecific digestion of the MB can occur [103]. Another way to try to lower the LOD of immobilized MBs is to use light guiding NWs as substrate, as was done here, in project 3.

4.1.3 Lightguiding NWs

It has been shown that semiconducting NWs can be used for signal enhancement [36], [38]. The materials building up the NWs need to have high refractive index, and the diameter of the NW has to be optimized. When fluorescent molecules bind to the surface of these semiconductor NWs, light gets coupled in the NW core, resulting in a directional emission from the NW extremities [104]. Studies have shown that when fluorescently labeled streptavidin is attached to a SiO₂ coated NW using biotin, the light guiding effect is comparable for NWs grown using epitaxy and aerotaxy [105], and the signal enhancement of labelled streptavidin results in a lowered LOD of the molecule.

In project 3, the probing benefits of MBs are combined with light guiding effect of semiconducting NWs to improve the detection of DNA oligonucleotides in solution, see schematic in figure 16. Immobilization of the MBs through layer-by-layer buildup is performed in a microchannel by flowing PLL-g-PEG molecules, streptavidin, a biotinylated DNA tether, and the MB itself, over a NW platform. In order for the MB to link to the biotinylated DNA tether, the MB was designed with an extra sequence, complementary to the DNA tether, on the quencher end. A complementary oligonucleotide is then introduced in the solution and the fluorescence is observed over time using fluorescence microscopy.

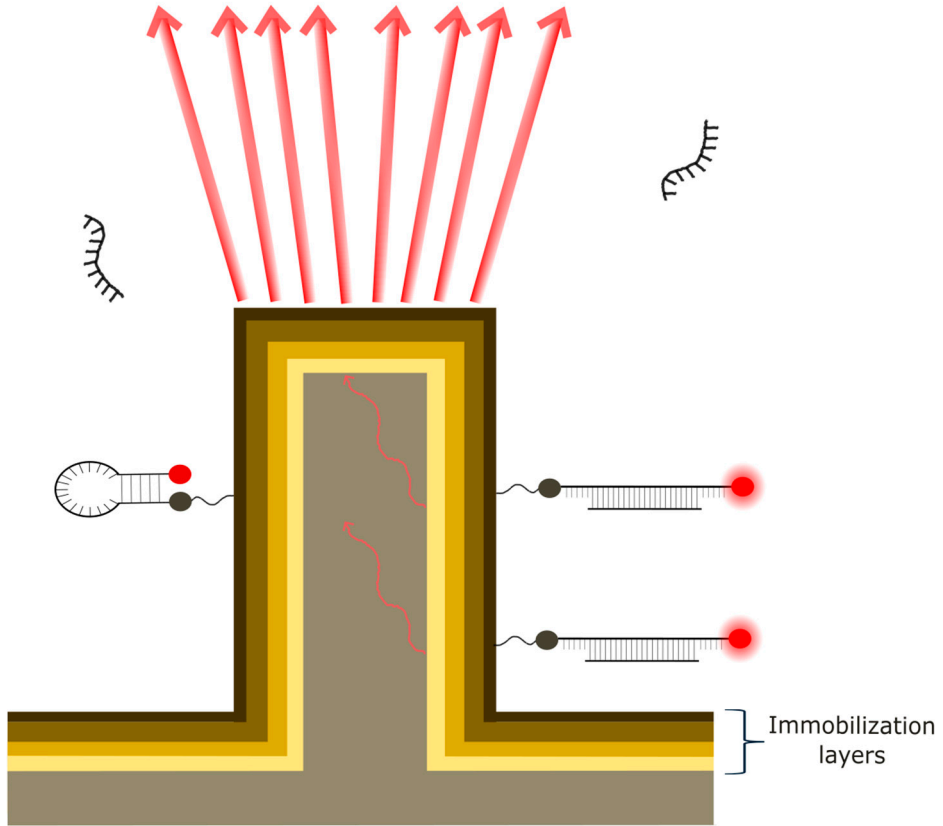


Figure 16. Lightguiding effect in NWs. When a MB immobilized on the NW surface hybridize with a complementary oligonucleotide, the beacons emits a fluorescence signal, which is transported through the NW and emitted directionally from the top of the NW.

4.2 Results

4.2.1 Functionality of NWs

The ABL1 gene was chosen as the target for the MB design. The designed MB had the sequence TAT TTC TGA TGT CCA CCC CC/TAO/GCT GGC ACG TTA ACA AAA GGA AGG GAC CAG C/ATTO647N/, where letters in bold are the loop sequence that is complementary to nucleotide 6 to 30 in the ABL1 mRNA, letters in italic are the stem, ATTO647N is the fluorescent dye, and TAO is the

quencher. The underlined letters are the extra DNA sequence that is attached to act as anchor for the MB to the NW substrate.

In order to test their functionality, the MBs were mixed in solution with a complementary oligonucleotide, or a scrambled control oligonucleotide, using a fluorescence plate reader, see figure 17. When adding complementary oligonucleotide to the MBs, an increase in fluorescence is observed, indicating hybridization between MBs and complementary oligonucleotides. The fluorescence also increased with increasing complementary target concentration, up to a target concentration of 500 nM where the signal becomes saturated. A high concentration of 1 μ M scrambled oligonucleotide did not give an increase in fluorescence compared to background. These results suggests that the MB is efficiently designed, and that the MB is functional and selective.

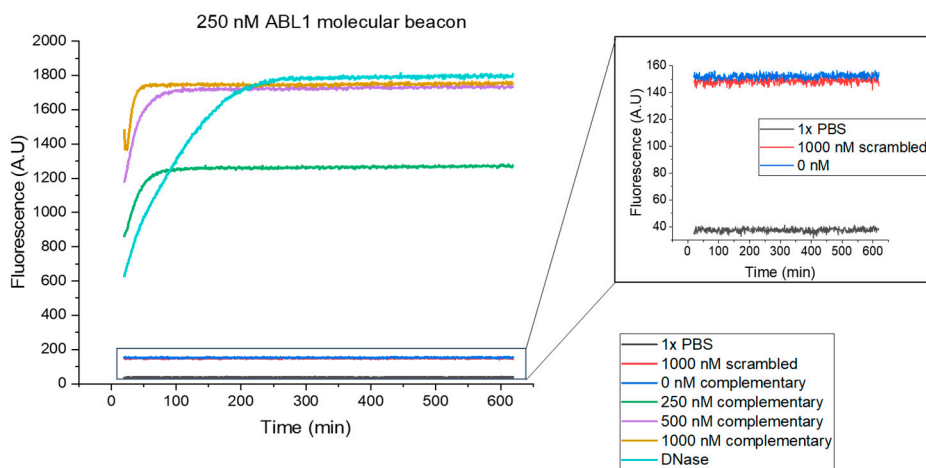


Figure 17. MB fluorescence in solution. Plate reader measurements showing fluorescence intensity of MBs in 1x PBS over time when introduced to different concentrations of complementary oligonucleotide target. A scrambled oligonucleotide was added as control. Inset shows zoom-in for MB fluorescence background (0 nM oligonucleotide), 1x PBS, and MBs together with high concentration of scrambled oligonucleotides.

4.2.2 Detection of complementary oligonucleotides on the NW platform

Using light guiding NWs as substrate for MB immobilization is a possible way of lowering the LOD for complementary oligonucleotides, which we explored in project 3. ABL1 MBs were immobilized on a NW substrate and complementary oligonucleotides of increasing concentration were added to the device. The fluorescence change over time for individual NWs was registered to investigate the LOD of the oligonucleotide using the MBs. For NW with increasing intensities

over time, the average line coefficient k was assessed ($\Delta I(\text{A.U})/\text{minute}$). An increase in complementary oligonucleotide concentration resulted in an increase in number of NWs with increasing fluorescence over time, starting at complementary target concentration 0.1 nM, see figure 18A. This suggests that the LOD of the setup is 0.1 nM. The large proportion of more than 70% NWs with decreasing fluorescence at complementary oligonucleotide 0 nM, is speculated to be due to bleaching and MBs remaining in solution after washing at the beginning of the experiment.

The average line coefficient of nanowire with increasing intensities k , is increasing with complementary oligonucleotide concentration (Figure 18B), suggesting that not only the number of NWs with increasing intensity getting larger, but the speed at which this happens is also higher. This is also mirrored in the sum intensity of the NWs with increasing fluorescence at different complementary oligonucleotide concentrations (Figure 18C).

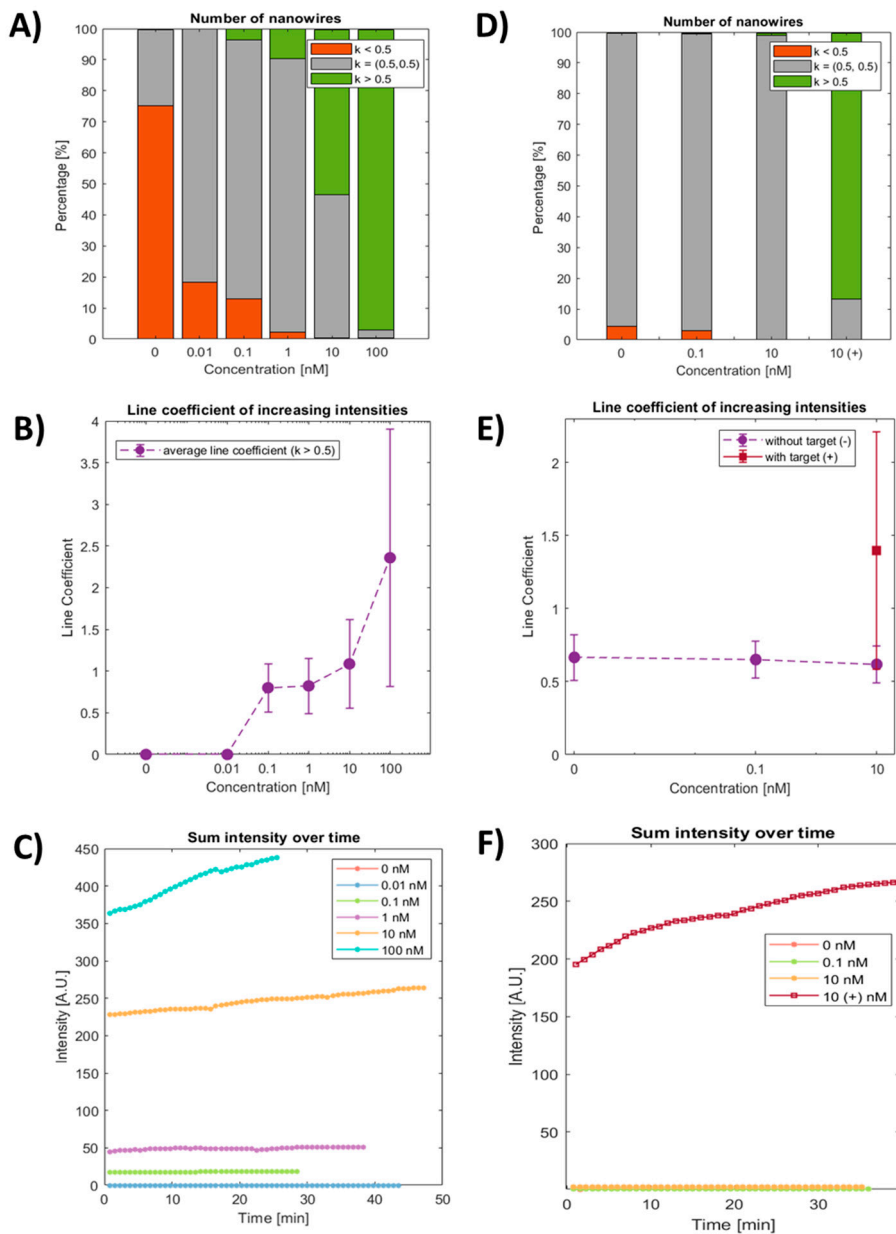


Figure 18. Detection of MB fluorescence when a complementary oligonucleotide is introduced to MBs immobilized on GaP NWs (A-C), or to a scrambled control oligonucleotide (D-F). A, D) Distribution of NWs with increasing (green), decreasing (red), and stationary (gray) fluorescence signal at different oligonucleotide concentrations. B, E) Line coefficient of fluorescence over time for NWs with signal in (A, D). At the end of the control experiment in (E-F), 10 nM complementary oligonucleotide was added to the NW platform as an extra control of the system C, F) Sum intensity over time for NWs with increasing fluorescence $k > 0.5 \Delta I(\text{A.U.})/\text{minute}$ for different complementary oligonucleotide concentrations (C), or complementary and scrambled oligonucleotide (F).

As a control, the experiments with the immobilized MBs were repeated with a scrambled oligonucleotide. It was clear that introducing the scrambled oligonucleotide did not cause an increase in MB fluorescence (Figure 18D-F). This supports the fact that the MB is selective to the ABL1 gene sequence. As an extra control, 10 nM complementary oligonucleotide was added to the platform at the end of the control experiment to make sure that the lack of fluorescence increase was not due to a defect platform.

At the beginning of the control experiment (at 0 nM scrambled oligonucleotide), the proportion of NWs with decreasing fluorescence signal was only a few percent (Figure 18D), compared to 70% for the experiment with complementary oligonucleotide. This difference is probably related to variations between individual samples, such as contamination or unintentional tilt of the platform.

In summary, fluorescence plate reader measurements indicated that the ABL1 MBs had been designed to successfully hybridize with complementary oligonucleotides. We have shown that it is possible to detect complementary oligonucleotides using ABL1 MBs immobilized on NWs, with a LOD of 0.1 nM. Below 0.1 nM, only NWs with decreasing or stationary fluorescence signal were observed. Control experiments with scrambled oligonucleotides did not show any increase in fluorescence.

Our results shows an alternative way of probing molecules using immobilized MBs. Other studies have previously investigated MBs immobilized on different surfaces, as a way for reaching a better sensibility and LOD, and with varying results. There have been studies showing that the hybridization efficiency varies for different MB coverages on the surface [106]. For MB coverage in the range between 0.3×10^{12} MB/cm² and 1.2×10^{12} MB/cm², the hybridization efficiency increases with increasing coverage, followed by a efficiency drop from 90% to approximately 20% when the MB surface coverage is higher than 1.2×10^{12} MB/cm². In our case, the coverage density of the MBs is estimated to be approximately 1.4×10^{11} MB/cm², suggesting that the hybridization efficiency could be increased if the coverage density could be increased.

The LOD for complementary oligonucleotides on immobilized NWs in project 3 was 0.1 nM. This is lower than the LOD presented by Lui and Tan in a somewhat similar setup [107]. By immobilizing biotinylated MBs on an optical fiber core, they showed a LOD of 1.1 nM. Studies have also been performed where MBs were immobilized on a gold surface in order to investigate the quenching effect of gold instead of using a separate quencher [108]. In that study, the LOD was determined to be 10 nM.

There are also setups showing a lower LOD than what could be reached in project 3. One example is the use of paper-based lateral flow strips that have been reported to reach a LOD down to sub femtomolar for immobilized MBs detecting target nucleic acids [101]. This technique uses pads that pull a sample liquid over a test

line with stationary MBs. The result can then be evaluated using fluorescence microscopy. Despite the low LOD, there are some drawbacks to this on-site diagnostics, such as long preparation times for the devices and the use of multiple chemical steps.

Despite the LOD achieved in project 3 not being the lowest registered, the setup is still a promising alternative to current methods using immobilized MBs. The light guiding effect eliminates the need for amplifying the target prior to measurements, and also makes it possible to probe complex samples, without the need of using transparent liquids since the signal is gathered at the NW extremities.

One drawback of our setup, in its current form, is the high cost related to NW fabrication requiring expensive substrates and the cost of MOVPE growth. However, it has been shown that the lightguiding properties are present both for NWs grown using epitaxy and aerotaxi [105]. This opens for the opportunity to use aerotaxi NWs in the future and thereby lowering the costs, since substrate cost would be eliminated and the process is less expensive [105]. The solution volumes used in the setup are also relatively large, which can be both costly and make it hard to detect rare agents. Here, further development of the sample chambers needs to be done to minimize the volumes needed.

Within the scope of project 3, MBs designed to target part of the ABL1 gene were immobilized on light guiding NWs and used for detecting complementary oligonucleotides, with a LOD of 0.1 nM. The setup is promising as an alternative to existing methods, and by using aerotaxy grown NWs and developing the sample chamber size, costs can be further decreased compared to the setup in its current form.

5 Experimental methods

In this section, I will briefly describe the techniques that have been of importance during my thesis work. It will also be stated in which project(s) the method has been used.

5.1 NW synthesis and characterization

The NWs used in project 1 were photovoltaic Indium phosphide (InP) NWs of p-i-n and inactive type. The fabrication and characterization of the NWs were performed by Lukas Hrachowina at the division of Solid State Physics, Lund University. The NWs were grown in the Lund Nano Lab (LNL), using metalorganic vapor phase epitaxy (MOVPE). In order to check the electrical properties of the p-i-n-junction, electron beam-induced current (EBIC) was performed. Some of the NWs were also coated with silicon dioxide (SiO₂) using atomic layer deposition (ALD) to act as a control for the optoelectronic properties. All NWs were imaged using scanning electron microscopy (SEM) to make sure they had suitable length, diameter and shape.

In project 3, lightguiding Gallium phosphide (GaP) NWs were used. These were fabricated and characterized by Aligned Bio AB in the LNL, using MOVPE and SiO₂ ALD coating. SEM was used for characterizing the NWs after growth.

5.1.1 Metalorganic vapor phase epitaxy (MOVPE)

Metalorganic vapour phase epitaxy (MOVPE) is a vapor deposition method to create crystalline structures or films. Prior to MOVPE growth, Au catalyst particles are added to the substrate. In our case this was done using nano imprint lithography (project 1) or displacement Talbot lithography (project 3). The substrate was placed in the MOVPE reactor chamber and precursors in vapour phase were introduced in the chamber. The different precursors used to fabricate the wires in project 1 were phosphine (PH₃), trimethylindium (TMIn), diethylzinc (DEZn) and tetraethyltin (TESn). For the NW fabrication in project 3, trimethylgallium (TMGa) and PH₃ were used as precursors. The precursors accumulate in the liquid catalyst particle until it is saturated. The precursor then enables the growth of a wire by crystalizing

at the particle-substrate interface [109]. As long as the flow of precursors is on, the wire will continue to grow. A simplified schematic of the MOVPE process is shown in figure 19.

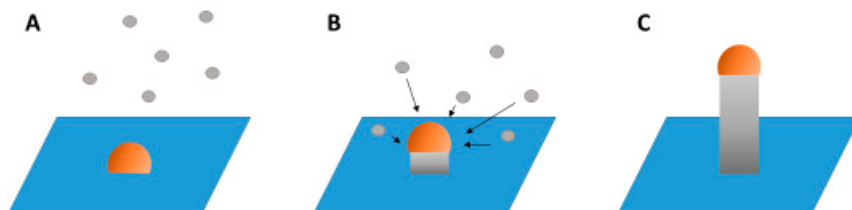


Figure 19. Simplified schematic of NW growth through MOVPE. (A) Au nanoparticles are seeded on a substrate and get exposed to precursors (illustrated as gray dots) in the MOVPE growth chamber. (B) The precursors enter the liquid Au particle and when the particle is saturated a NW will start to form underneath it. (C) The growth ends when the flow of precursors stops.

5.1.2 Atomic layer deposition (ALD)

Atomic layer deposition (ALD) is a method for creating thin films one atomic layer at the time [110]. The substrate or structure one wishes to coat is placed in an ALD chamber. Precursor molecules will enable the buildup of an atomic layer. An inert carrier gas help venting the chamber and the pressure in the chamber is kept low to avoid contamination [111]. ALD was used to coat the NWs with SiO_2 in project 1 and project 3.

Already before any coating starts, the structure has hydroxyl groups connected to its surface [112]. As the first precursor is introduced in the chamber, the precursor molecules react with the hydroxyl groups and thereby bind to the surface. Byproducts are formed and are vented from the chamber together with the excess precursor. When the second precursor then is introduced it will react with the molecules at the surface, completing the first atomic layer [111]. The second precursor can also be exchanged by a plasma step where radicals react with the surface. Since the plasma is more reactive compared to the precursors, the process can be performed at lower temperature [113], [114]. By repeating this whole cycle, one can create layers of controlled thickness. The layer will continue to grow thicker as long as the cycles are repeated. Figure 20 shows a simplified schematic of one cycle in the ALD process.

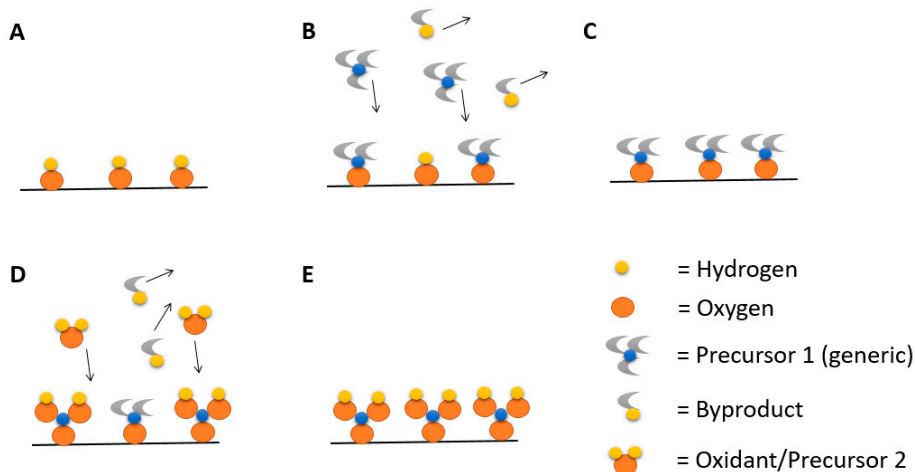


Figure 20. Simplified schematic of ALD. (A) Oxide layer on the surface before ALD starts. (B) Flow of first precursor that interacts with the surface. (C) Excess precursors and byproducts are vented from the chamber. (D) Flow of oxidants that interact with the surface. (E) Excess oxidants and byproducts are vented from the chamber. The top molecules in the layer is now the same as in (A) and the cycle can be repeated if desired.

5.1.3 Scanning electron microscopy (SEM)

Scanning electron microscopy (SEM) is a suitable tool for characterizing the length and shape of the fabricated NWs. The electron beam is generated by an electron gun and vacuum is needed to avoid contamination and to obtain high resolution [115]. Electromagnetic lenses are used to focus the electron beam, and scanning coils enable the beam to do a scanning motion along the x- and y-axis across the sample [116].

Incident electrons in the focused electron beam interact with the atoms in the sample, giving rise to different kinds of signals that can be collected by detectors, see figure 21. Secondary electrons are low energy electrons originating from the sample. Electrons in the incoming electron beam have interacted with these sample electrons and transferred enough energy to them for the sample electrons to leave the sample. Secondary electrons are good for studying the topography of the sample [117]. Backscattered electrons, on the other hand, are incident electrons that reached deeper into the sample, there interacting elastically before leaving the sample. They are useful for studying composition [118]. In project 1 and project 3, SEM was used to characterize NWs after growth. In project 2, nanostraws were imaged using SEM.

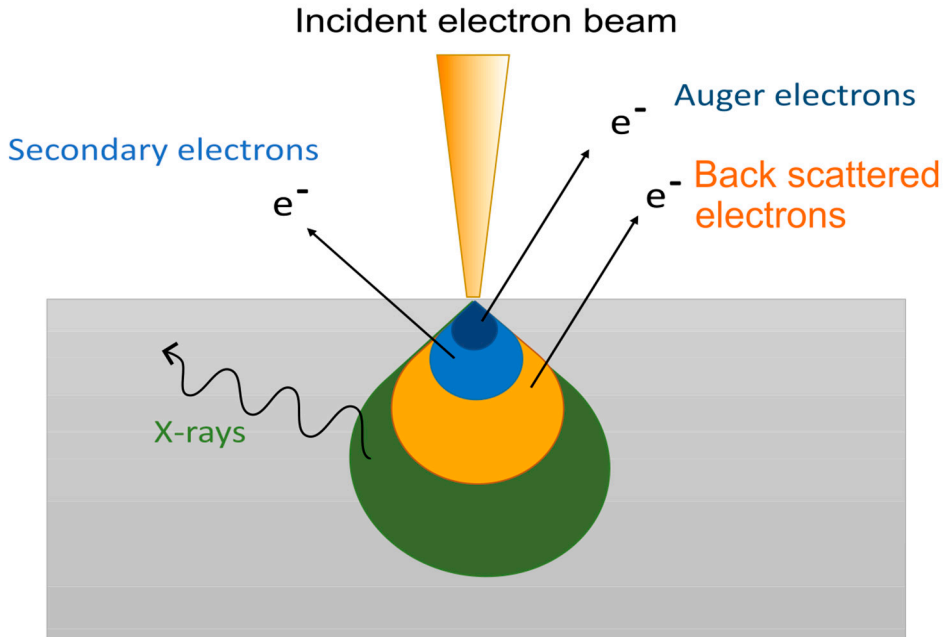


Figure 21. Different origin of signals detected in SEM. Different kind of X-rays origin from deeper layers of the material (green section). Auger electrons originate from the dark blue section. However, in this thesis work, only secondary and backscattered electrons were of interest.

5.1.4 Electron beam-induced current (EBIC)

Electron beam-induced current (EBIC) is a technique for analysing junctions and defects in semiconductors [119]. This can be performed in a SEM. The electron beam generates electron-hole pairs in the illuminated structure and the generated current is then measured. By swiping with the electron beam over a NW structure and measuring the current, one can get data about the p-n junction properties [120].

5.2 Cells

During the work on this thesis, cells lines have been used to investigate the effect of illuminated photovoltaic NWs (project 1) and to study the fate of injected molecular beacons into cells (project 2). The cells used in project 1 are A549 lung cancer cell line, acquired from the European Collection of Cell Cultures (ECCC, distributor Sigma Aldrich). All experiments were performed using cells between passage 96 and 101. The cells used in project 2 are INS-1 rat insulinoma cells [121] (beta cells) at cell division number 50-60.

5.2.1 Cell culture

In project 1, A549 lung cancer cells were thawed and seeded in T-25 or T-75 cell culturing flasks in Ham's F12K medium supplemented with fetal bovine serum (FBS) and penicillin-streptomycin. The medium was then changed every second day until 80% confluency was reached. When the cells were ready to be seeded on NW substrates, they were washed with Dulbecco's phosphate buffered saline (DPBS), trypsinized and centrifuged. The supernatant was removed and the cells were resuspended in fresh medium, counted and finally seeded on sterilized InP NW samples. After seeding the cells, the next step is to expose the cells and NWs to dark or light conditions.

In project 2, beta cells were thawed and cultured in T-25 cell culturing flasks in RPMI-1640 medium supplemented with heat inactivated FBS, penicillin-streptomycin, HEPES solution, and INS-1 supplement (solution of glutamine, Na-pyruvate, and 2-mercaptoethanol). The culturing medium was exchanged every second day, and when the cells had reached 80% confluency, they were washed and trypsinized the same way as the A549 cells. After resuspension, the counted beta cells were seeded on sterilized nanostraws, before being exposed to nanoelectroporation.

5.2.2 Illumination of cells and photovoltaic NWs

In project 1, cells were seeded on NWs and placed in black boxes in a 37 °C, 5% CO₂ incubator and cultured for 48h. The black boxes are designed to isolate the cell culture from external light. In one of the boxes, an electroluminescent light panel was installed. During 48h, some cells were in a constantly dark box (control) and some in a box with constant illumination from the light panel.

To investigate whether the cell population recovered after illumination, cells were kept in the boxes for 48h in dark or light conditions and then cultured for another 48h in the dark. After 48h (or 48+48h for recovery experiments), cells were fixed with 4% paraformaldehyde (PFA) prior to labeling and imaging.

5.3 Nanostraws

Nanostraws were used together with nanoelectroporation in project 2 for injection of MBs into beta cells. After fabrication the nanostraw membrane was attached to a cylinder as described below.

5.3.1 Nanostraw fabrication

The nanostraws used in project 2 were fabricated in the LNL by Diogo Volpati and Frida Ekstrand from the division of Solid State Physics, Lund University. Polycarbonate (PC) membranes with 200 nm diameter nanopores are used as base for the nanostraw fabrication in project 2. The membranes are coated with approximately 12 nm alumina using ALD. For removal of horizontal alumina on the membrane, inductively coupled plasma and reactive ion etching (ICP-RIE) is used, followed by another step of ICP-RIE to etch underlying PC. After 1 μm of PC is etched away, nanostraws will protrude from the PC membrane.

5.3.2 Nanoelectroporation

To open up the cell membrane and transport MBs into the cytosol, nanoelectroporation was used in project 2. The droplet of the MB solution in MilliQ water is placed on a flat gold electrode and the nanostraw membrane with seeded cells is placed on top, see figure 22. A platinum top electrode is inserted in the medium above the cells, with a inter electrode distance of 0.5 mm. The nanoelectroporation is performed by applying square pulses at 40 Hz, 20-28 V in amplitude, with a pulse duration of 200 μs , in total 2 pulse series of 40 seconds each. The result of the injection is then imaged using flow cytometer or fluorescence microscope, which are described in the following sections.

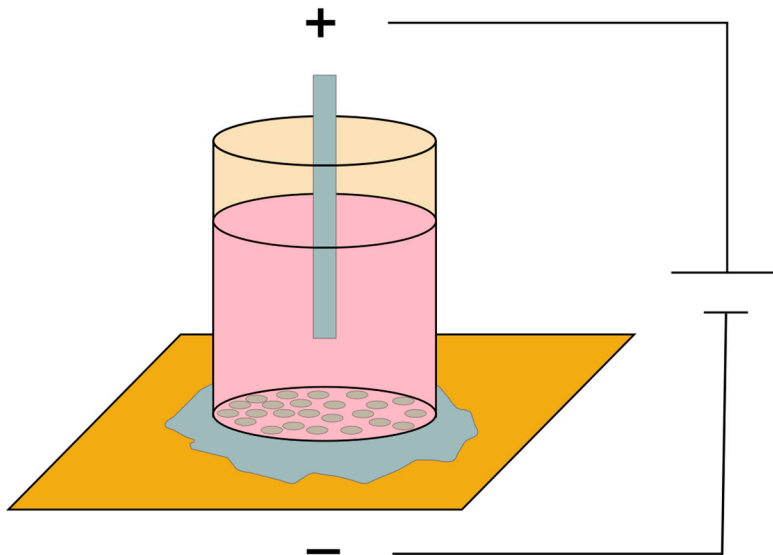


Figure 22. Schematic for nanoelectroporation setup. A nanostraw membrane is attached to the bottom of the cylinder, and MBs are injected to the beta cells seeded on the membrane.

5.4 Fluorescence

Fluorescence is the ability of an atom or a molecule to emit light of a certain wavelength after being exposed to light of a shorter wavelength. Incoming photons with high enough energy excite the fluorescent molecule from the ground state to an excited state, see left part of figure 23. Energy loss through heat dissipation then occurs when it relaxes down to the lowest level of the excited state. Consequently, when the excited molecule returns to its ground state, a photon is emitted with a lower energy than the energy of the incoming photon, a phenomena known as Stokes shift. Since more than one excitation energy and emission energy is possible, a spectrum of excitation wavelengths and emission wavelengths can be observed, see right part of figure 23 [122]. Fluorescence is a useful and highly used tool for detection and monitoring of biomolecules, especially inside of cells. When performing fluorescence labelling and fluorescence microscopy of different kinds, it is important to choose a dye molecule with suitable excitation and emission spectra with respect to light sources and filters available, in order to optimize the fluorescent signal.

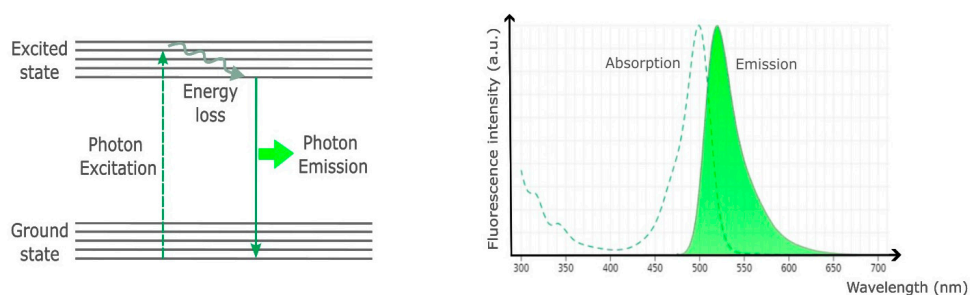


Figure 23. Stokes shift in fluorescence. Left: Jablonski diagram showing photon excitation leading to lower energy photon emission. The Stoke shift is due to energy losses during relaxation. Right: Stoke shift giving rise to shifted wavelength spectra for excitation and emission, here for Alexa Fluor 488 dye as an example.

5.4.1 Fluorescence microscopy

With a fluorescence microscope (see figure 24), it is possible to see fluorescently labelled structures or proteins in cells. A light source sends light into the filter cube of the microscope. The filter cube contains an excitation filter, a dichroic mirror and an emission filter. Depending on which wavelengths are transmitted through the different filters and the dichroic mirror, different fluorophores can be visualized. The excitation filter transmits a specific wavelength used to excite the fluorophore and a dichroic mirror reflects that light towards the sample. When excited, the fluorophore emits light of a longer wavelength, which is transported back and transmitted through the dichroic mirror. An emission filter makes sure that only the

emitted light from the sample reaches the detector or eyepiece. Fluorescence microscopy was used in project 1, projekt 2, and project 3.

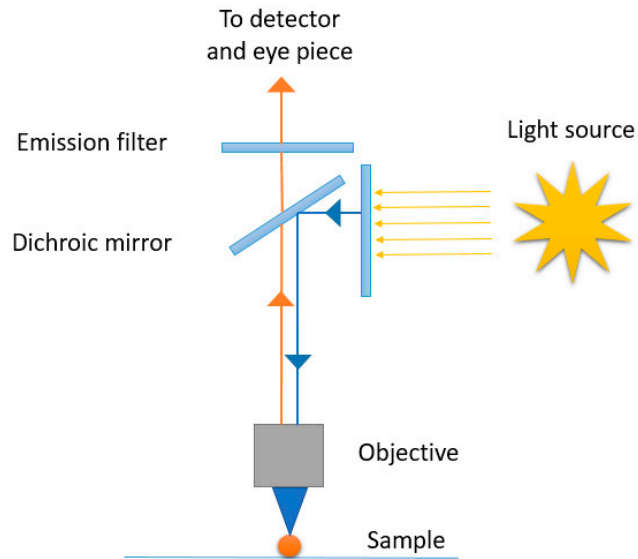


Figure 24. Simplified schematic of a fluorescence microscopy setup.

5.4.2 Fluorescence labelling

In project 1, two different types of fluorescence labelling were used prior to fluorescence microscopy imaging; anti-Ki67 and TUNEL. All cells were also counterstained with Hoechst. In project 2, Hoechst, Lysotracker, and Mitotracker were used to stain the cells.

5.4.2.1 *Anti-Ki67*

Ki67 is a nuclear protein present in all active cells, i.e. all cells that are not in the G_0 state. It is a marker for cell proliferation and is therefore often used in cancer investigations, since an increased level of Ki67 can predict tumour growth and metastasis [123]. Anti-Ki67 is a primary antibody that binds to Ki67. In project 1, when investigating whether or not the cells were in an active state at the time of culture termination, the fixed cells were washed with DPBS and permeabilized before the primary anti-Ki67 antibody was added. After incubation and washing of the cells, a secondary antibody connected to the fluorescent dye AlexaFluor 488 was added. The cells were then washed again.

5.4.2.2 *TUNEL*

Terminal deoxynucleotidyl transferase dUTP nick end labeling (TUNEL) is an assay for detecting apoptosis in cells. Apoptosis is programmed cell death as a step in early development, normal cell turnover in aging, or as a result of other cell damage beyond repair. A cascade of events leads to cell shutdown, including degradation of proteins and fragmentation of DNA [124]. The TUNEL assay act by binding to the 3'-hydroxyl termini of fragmented DNA [125]. In project 1, the fixed cells were permeabilized followed by incubation with the TUNEL solution. The cells were then washed. Only one incubation step is needed since the TUNEL also carries a fluorescent dye itself.

5.4.2.3 *Lysotracker*

Lysosomes are enzyme containing organelles in the cell, responsible for breaking down molecules from both inside the cell, and taken up from the environment [126]. Lysotracker is a hydrophobic weak base that easily accumulates in acidic vesicular compartments. This makes it a useful fluorescent probe to stain lysosomes in cells. Due to its hydrophobic properties, Lysotracker can enter the cell through diffusion. After entering the lysosomes, it gets protonated which adds on to the confinement of Lysotracker in the lysosomes [127]. In project 2, Lysotracker is added directly or 24 hours after nanoelectroporation to live cells seeded on nanostraws. After 1.5 hours of incubation, the cells are washed.

5.4.2.4 *Mitotracker*

Mitochondria are organelles with a negative membrane potential. They produce most of the chemical energy needed in the cell. Due to cationic properties, Mitotracker, which is a fluorescent probe, accumulate in the mitochondria. [127]. Mitotracker is in our case added 24 hours after nanoelectroporation to live cells seeded on nanostraws in project 2. The incubation time is 30 minutes, and rinsing with DPBS is then performed.

5.4.2.5 *Hoechst*

Hoechst is a non-intercalated dye which binds to the outside of the double stranded DNA at A-T rich sections. It is cell permeable due to the presence of a lipophilic ethyl group and can stain the DNA in the nucleus of both live and dead cells [128]. This allows to clarify the location of cells, or counting the total number of cells. Hoechst is often used in co-staining together with other fluorescent dyes. In our case, it was used to label both fixed cells together with anti-Ki67 and TUNEL assay (project 1), and live cells together with Lysotracker and Mitotracker (project 2). The incubation time for Hoechst is 2 minutes, prior to the solution being rinsed away with DPBS.

5.4.3 Fluorescence plate reader measurements

A fluorescence plate reader is a tool for measuring fluorescence samples in 96 well plates. Similar to fluorescence microscopy described above, a light source illuminate the sample through an excitation filter, selecting a suitable wavelength for the fluorophore present in the sample (see figure 25). The excitation light scans over the well plate containing the sample. These scans can be repeated in order to monitor fluorescence over time. The fluorescence light emitted from the samples goes through an emission filter towards a photomultiplier tube (PMT detector) where the signal from each well is amplified in the software.

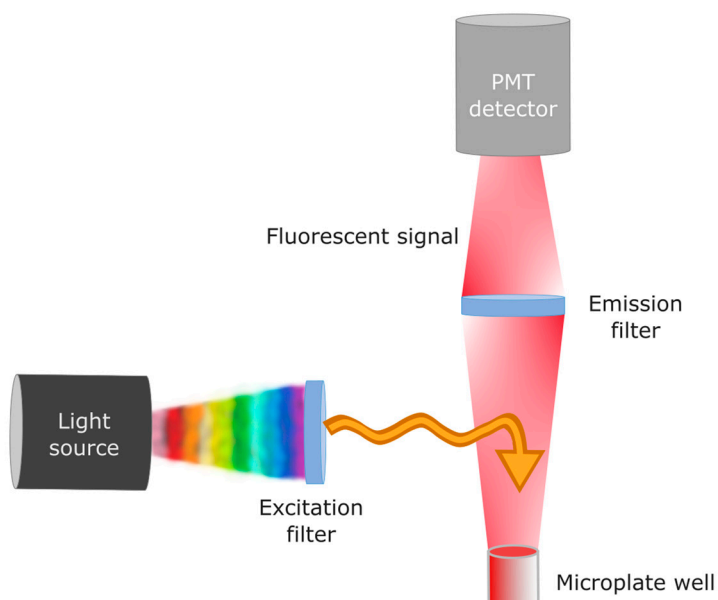


Figure 25. Simplified schematics of a basic fluorescence plate reader.

In both project 2 and project 3, the functionality of the MBs were tested using fluorescence plate reader measurements. To perform these measurements, the MBs are diluted in different concentrations of DPBS. The diluted MBs are pipetted into the wells of a 96-well plate and a complementary oligonucleotide sequence is added as a target. A scrambled oligonucleotide sequence is used as a specificity control, and to estimate the maximum signal, DNase, which degrades the MBs, is added to the MB solution. During the experiments in this thesis work, I have been using a CLARIOstar plate reader (BMG Labtech).

5.4.4 Flow cytometry

Flow cytometry is an analysis technique where cells in solution run through a laser beam to provide information about multiple parameters of the cell. By lining up the cells in a micro channel, the cells will be hit by the laser one at a time, giving information about individual cells and making it possible to use for cell counting (see figure 26). Even without any labelling, size and granularity can be assessed for cells run through flow cytometry. Forward scattering gives an estimation about the cell size, while side scattering tells us about the intracellular complexity [96]. If the cells are fluorescently labeled prior to flow cytometry, the fluorescent signal can be detected [95]. Multiple fluorescent markers can be used simultaneously, as long as the excitation and emission of the markers do not overlap too much between different fluorophores.

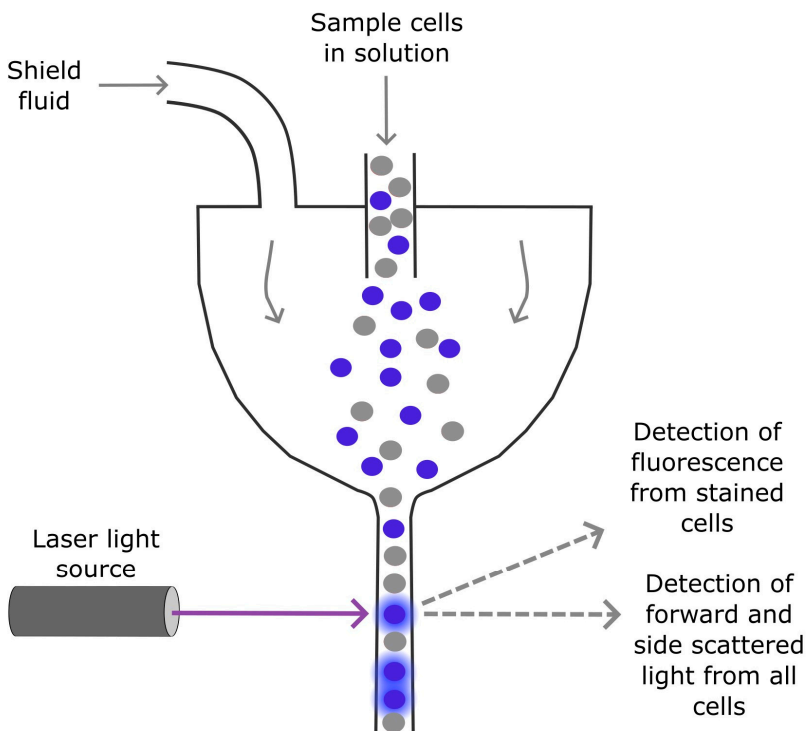


Figure 26. Simplified schematics of a flow cytometry setup.

5.5 Molecular beacons

In project 2 and 3, MBs were used as detection probes. Below is a brief summary of how they were designed and detected.

5.5.1 MB design

The selection and design of the MBs were performed by Roberto Munita at the division of molecular hematology, Lund University, and Diogo Volpati at the division of Solid State Physics, Lund University.

The database National Center for Biotechnology Information [129], [130] was used to find the gene of interest and the corresponding mRNA sequence. In project 2, the mRNA for the gene *Ins1* has been chosen as the investigated gene transcript. In live human beta cells, this mRNA is a precursor of the hormone insulin. In project 3, the mRNA for the gene ABL1 was chosen.

The MB loop should consist of ≈ 20 nucleotides, which is a small fraction of the number of nucleotides in the mRNA. Therefore, once a gene has been identified one needs to choose a target region along the mRNA. This sequence needs to be available for the MB loop to hybridize to, and therefore it should not be self-hybridized, which is checked for by using the RNAfold web server [131].

The chosen sequences in both project 2 and project 3, also had to be checked against other genes to make sure we have a unique section that could be used in the MB design with high selectivity. This was done by using the Basic Local Alignment Search Tool (BLAST) [132]. The Freiburg RNA tools [133] and the Integrated DNA Technologies (IDT) website [134] were then used to optimize the MB secondary structure regarding stability, melting temperature, folding and self-hybridization.

For MBs used in project 3, an extra sequence was added to the quencher end of the beacon. This extra sequence is used as an anchor to a complementary DNA surface tether when the MB is immobilized to the NWs.

When a suitable molecular beacon has been identified, a first step in investigating its stability and efficiency is to do fluorescence plate reader measurements where the beacons are introduced to complementary nucleic acid sequences instead of the full length mRNA it is targeting.

5.5.2 Immobilization of MBs

Immobilization of MBs in project 3 was carried out using a special designed NW platform where multiple immobilization layers had been added. The NW platform was fabricated using polydimethylsiloxane (PDMS) and soft lithography. Together

with a curing agent, the PDMS is cured on a silicon/tape template. Plasma treatment of the PDMS and a glass slide lead to silanol groups forming, causing the surfaces to react immediately when put in contact, attaching to each other [135]. Before sealing the device, a GaP NW array was attached in the microchannel. Holes are then punched in the PDMS to create inlet and outlet of the device, and reservoirs of 300 μ l are attached to these. To avoid unspecific binding, the device was passivated using Poly-L-Lysine grafted Polyethylene Glycol (PLL-g-PEG) before use. All solutions were administered to the NWs by negative pressure through capillary tubing, using a syringe pump. After passivation, the immobilization layers are created through layer-by-layer buildup, consisting of PLL-g-PEG with and without biotin (2% of total PLL consisted of 50% biotinylated PLL), streptavidin, biotinylated DNA tether, and finally the MBs themselves. When designing the MBs, an extra nucleotide sequence was added, which is complementary to the DNA tether, enabling the MB to attach to the surface. The flow of liquid in the device was kept constant and every new layer was incubated for an hour before being rinsed with DPBS. Administration of complementary oligonucleotides was performed the same way as for the immobilization layers.

5.6 Data analysis

In project 1, the percentage of TUNEL positive cells and Ki67 positive cells were manually counted by comparing fluorescence microscopy images showing TUNEL or anti-Ki67 labelling with images showing Hoechst. For statistical analysis, one-way analysis of variance (ANOVA) together with Tukey test for pair-wise comparison was used. All results were finally visualized in graphs using the OriginPro software.

In project 2 and project 3, fluorescence data was exported from the fluorescence plate reader software and visualized in graphs using Excel and the OriginPro software. In project 2, graphs were produced using flow cytometry data and ImageJ on microscopy images. The result was visualized using Excel and GraphPad.

In project 3, the fluorescence microscopy images were run through software NanoLoki, developed by Rubina Davtyan at division of Solid State Physics, Lund University. For every oligonucleotide target concentration, the location of each individual NW was detected by averaging all images over time. Then the fluorescence intensity for each NW was registered over time. After doing linear fits and observing the intensity slope for each NW, intensity plots were made in Matlab only for NWs with increased fluorescence signal.

6 Concluding remarks and Outlook

In this thesis, I have investigated how nanotools, such as MBs, NWs and nanostraws, can be used to manipulate and enable probing of cells. MBs were also used to detect oligonucleotides in solution. In this chapter, I will give some concluding remarks and outlook for the three main projects presented.

6.1 Photovoltaic NWs as dormancy switch

Although NWs have been used in biosensing and as cell substrate, it has not been investigated how cells react to interacting with illuminated photovoltaic NWs. This is the scope of project 1 in this thesis. Cells were seeded on InP photovoltaic NWs and then illuminated. Light absorbed by the p-i-n NWs resulted in a current that affected the cells and made them enter dormancy. Control cells seeded on the same type of photovoltaic NWs, but not exposed to illumination, showed less tendency of entering dormancy. Control experiments were also executed to show that the cells were dormant and not dying, and to show that the decreased proportion of active (non-dormant) cells was not due to topography, phototoxicity, or voltage build up.

These findings lead to the conclusion that p-i-n InP NWs in combination with light can be used to make cells enter dormancy in a controlled way, i.e. be used as a cell dormancy switch. This could be developed into a promising tool to create a model for studying dormancy in cells and how dormant cells react in different environments and in response to different treatments.

Compared to other cues that can induce dormancy, such as the extracellular matrix environment [136] and the addition of collagen [137], the advantages of the present setup is that the dormancy cue, i.e. the illumination of the NWs, is easy to control and, to our current knowledge, is not harming the cells.

The increased knowledge in functionality of dormant cells will be an important tool in research when developing and evaluating future cancer treatments. One possible continuation for this project is therefore to develop a chemotherapeutic compound not inducing dormancy or being effective also on dormant cancer cells, reducing the risk of non-effective treatment and reoccurring cancer. In order to minimize adverse effects of future cancer treatments, it is also of great importance to investigate more

cell types on the dormancy switch, including non-cancerous cells, to observe any variations in cell response.

6.2 Detection of *Ins1* mRNA using MBs and nanostraws

Multiple alternative techniques for detecting mRNA in cells are available, and although they often show a high sensitivity, they are not applicable to living cells. For methods such as microarray assays, northern blot and Ribonuclease protection assay, killing of the cells is needed to extract the mRNA used in following detection steps. They also require large quantities of cells, even though it is often possible to combine the detection technique with an amplification step.

Using MBs for mRNA detection allows to keep the cells alive and longitudinal studies on live cells are therefore possible to achieve. Moreover, the MBs are not known to alter the function of the cells and many single cells can be analysed simultaneously, which make MBs an appealing tool for probing mRNA content in live cells.

The goal of project 2 was to investigate whether MBs could be used to detect *Ins1* mRNA in living beta cells. This corresponds to investigating the transcriptional state of live cells with respect to 1 gene, which, if proven valid, could be extended to 4 genes. To be able to do this is of importance in applications such as monitoring cell response to different internal and external stimuli, and to detect early stages of disease.

Initial bench tests to check MB functionality showed promising results. The MBs were exposed to a complementary oligonucleotide, which resulted in an increase in MB fluorescence due to hybridization between the two. Such increase could not be seen when the MBs instead was mixed with a scrambled oligonucleotide.

The MBs were then successfully injected into beta cells via nanoelectroporation using nanostraws, and time lapse fluorescence microscopy images showed that the MB fluorescence signal rapidly moved to the nucleus, followed by a translocation back to the cytosol, where the signal took a punctuated appearance. Cell labelling showed that MB signal colocalized with mitochondria, but not so much with lysosomes.

The benefits of using nanostraws for the MB delivery, in comparison with for example micro pipetting, are the facts that they are not harming the cells, and that it is possible to inject the MB cargo into a large number of cells simultaneously in a short time. However, although the delivery of the MBs into the cells was considered

successful, the fate of the MBs inside the cytosol is raising questions regarding the MBs suitability as mRNA probes.

Indeed, the results suggest that most of the MB fluorescence signal is actually false positive signal due to degradation or non-specific opening of the MBs, rather than hybridization. This makes the use of MBs problematic when trying to probe for mRNA inside of cells. Despite the negative results, the design of our experiments allow to shed light on the fate of MBs inside cells. By using nanostraws to inject MBs directly in the cytosol over a short time window, we were able to monitor the fluorescence signal and pinpoint the appearance of false positive signals, corresponding to degradation and/or non-specific MB opening in the nucleus.

Strategies to protect the MBs from degradation and nuclear translocation need to be further investigated, but without lowering the MB sensitivity for its target. The intracellular environment exposes the MBs to salts that may alter the behaviour of the MBs, and molecules such as nucleases that will degrade them. Some protection can be provided for the MBs if considering the stability already at the design step. There are studies showing that modifications such as methylation and addition of phosphorothioate can increase the stability of the MBs [86]. Similarly, several schemes have been developed to minimize nuclear sequestration, such as attaching tRNA or Neutravidin to the beacons to expel it from the nucleus, chemically modifying the beacon [138], or complex architectural modification of the beacons [139], [140]. However, with these modifications, it is still not clear whether this leads to fully functional beacons for reporting mRNA.

If one can overcome the degradation and the nuclear sequestration problems, using MBs could be a very promising tool to detect mRNA in cells, but meanwhile the risk of getting false positive signals is too large, resulting in misleading results.

6.3 Detection of oligonucleotides using MBs immobilized on light guiding NWs

The ability of detecting the presence of biomolecules in a solution using an immobilized probe is of great importance for biological applications, such as developing screening tests for different diseases. One candidate method for detecting oligonucleotides is the microarray assay. Both full genes, but also short DNA fractions can be immobilized on the microarray assay surface, acting as probes for their complementary nucleotide sequence. Another option is to use MBs.

The goal of my third project was to develop an alternative and more sensitive method to detect biomolecules, such as oligonucleotides. In this project, ABL1 MBs were immobilized on light guiding NWs mounted in a microchannel device. Complementary target oligonucleotides were then introduced to the MBs, resulting

in an increase in MB fluorescence for target concentration 0.1 nM and above. Controls with scrambled oligonucleotides instead of the target, showed no increase in fluorescence, indicating a successfully designed MB.

Although one of the aims was to decrease LOD for oligonucleotides, our results are comparable with other already existing studies [107]. Some speculations on why the detection was not more sensitive is that there is a balance between finding optimal settings with enough excitation of the MB fluorophore to get a clear signal, but at the same time avoiding excessive bleaching during laser exposure. Also, even though non-immobilized MBs are washed away before target is added, one could still assume there is a background signal from the immobilized MBs.

Despite this, our setup was shown to be another alternative to current techniques probing for biomolecules. Depending on what kind of information is desirable, different techniques can be of most interest. One advantage of MBs, is that they enable the detection of change in target hybridization over time, where microarray assays traditionally give a snapshot of the results at a certain time point.

While the microarray assay is capable of detecting a very large amount of genes simultaneously, the setup used in this project at present can only detect potentially a few oligonucleotides at the same time (limited by the color filters in the microscope). In the future, one can imagine achieving multiplexing by using a single fluorophore in MBs of different target sequences that are immobilized in different regions of the chip. This could be done using microfluidics or spotting of the NW substrate.

To further improve the sensitivity of the method, one could imagine exchanging the quencher and fluorophore positions, in order to have a fluorophore positioned closer to the NW surface and therefore increase the coupling of the MB fluorescence into the NW core. The MB background could also be lowered by increasing the number of nucleotides in the stem. This would have to be balanced with a possible corresponding decrease in hybridization with the complementary target. To lower the cost of the setup, using NWs grown using aerotaxy, instead of epitaxy, would be preferable. The device chamber also needs to be developed to efficiently handle smaller volumes, since the reagents are costly. When these aspects will have been taken care of, the technique will have the potential to develop into an alternative laboratory equipment for biomolecule detection. Some benefits with the technique are the controlled addition of volumes, and the signal enhancement due to the light guiding properties of the NWs.

7 References

- [1] R. Elnathan, M. Kwiat, F. Patolsky, and N. H. Voelcker, “Engineering vertically aligned semiconductor nanowire arrays for applications in the life sciences,” *Nano Today*, vol. 9, no. 2, pp. 172–196, Apr. 2014, doi: 10.1016/j.nantod.2014.04.001.
- [2] S. Bonde, N. Buch-Månson, K. R. Rostgaard, T. K. Andersen, T. Berthing, and K. L. Martinez, “Exploring arrays of vertical one-dimensional nanostructures for cellular investigations,” *Nanotechnology*, vol. 25, no. 36, p. 362001, Aug. 2014, doi: 10.1088/0957-4484/25/36/362001.
- [3] W. Hällström *et al.*, “Gallium Phosphide Nanowires as a Substrate for Cultured Neurons,” *Nano Lett.*, vol. 7, no. 10, pp. 2960–2965, Oct. 2007, doi: 10.1021/nl070728e.
- [4] T. Berthing, S. Bonde, C. B. Sørensen, P. Utiko, J. Nygård, and K. L. Martinez, “Intact mammalian cell function on semiconductor nanowire arrays: new perspectives for cell-based biosensing,” *Small*, vol. 7, no. 5, pp. 640–647, Mar. 2011, doi: 10.1002/sml.201001642.
- [5] S. Bonde *et al.*, “Tuning InAs nanowire density for HEK293 cell viability, adhesion, and morphology: perspectives for nanowire-based biosensors,” *ACS Appl Mater Interfaces*, vol. 5, no. 21, pp. 10510–10519, Nov. 2013, doi: 10.1021/am402070k.
- [6] K. S. Beckwith, S. Ullmann, J. Vinje, and P. Sikorski, “Influence of Nanopillar Arrays on Fibroblast Motility, Adhesion, and Migration Mechanisms,” *Small*, vol. 15, no. 43, p. 1902514, 2019, doi: 10.1002/sml.201902514.
- [7] J. B. Vinje, N. A. Guadagno, C. Progida, and P. Sikorski, “Analysis of Actin and Focal Adhesion Organisation in U2OS Cells on Polymer Nanostructures,” *Nanoscale Res Lett*, vol. 16, no. 1, p. 143, Sep. 2021, doi: 10.1186/s11671-021-03598-9.
- [8] H. Persson, Z. Li, J. O. Tegenfeldt, S. Oredsson, and C. N. Prinz, “From immobilized cells to motile cells on a bed-of-nails: effects of vertical nanowire array density on cell behaviour,” *Sci Rep*, vol. 5, p. 18535, Dec. 2015, doi: 10.1038/srep18535.
- [9] H. Persson *et al.*, “Fibroblasts Cultured on Nanowires Exhibit Low Motility, Impaired Cell Division, and DNA Damage,” *Small*, vol. 9, no. 23, pp. 4006–4016, Dec. 2013, doi: 10.1002/sml.201300644.
- [10] Z. Li, H. Persson, K. Adolffson, S. Oredsson, and C. N. Prinz, “Morphology of living cells cultured on nanowire arrays with varying nanowire densities and diameters,” *Sci China Life Sci*, vol. 61, no. 4, pp. 427–435, Apr. 2018, doi: 10.1007/s11427-017-9264-2.
- [11] A. K. Shalek *et al.*, “Vertical silicon nanowires as a universal platform for delivering biomolecules into living cells,” *Proceedings of the National Academy of Sciences*, vol. 107, no. 5, pp. 1870–1875, Feb. 2010, doi: 10.1073/pnas.0909350107.

- [12] N. Chevrier *et al.*, “Systematic discovery of TLR signaling components delineates viral-sensing circuits,” *Cell*, vol. 147, no. 4, pp. 853–867, Nov. 2011, doi: 10.1016/j.cell.2011.10.022.
- [13] N. Yosef *et al.*, “Dynamic regulatory network controlling TH17 cell differentiation,” *Nature*, vol. 496, no. 7446, Art. no. 7446, Apr. 2013, doi: 10.1038/nature11981.
- [14] L. Wang *et al.*, “Somatic mutation as a mechanism of Wnt/ β -catenin pathway activation in CLL,” *Blood*, vol. 124, no. 7, pp. 1089–1098, Aug. 2014, doi: 10.1182/blood-2014-01-552067.
- [15] F. Mumm, K. M. Beckwith, S. Bonde, K. L. Martinez, and P. Sikorski, “A transparent nanowire-based cell impalement device suitable for detailed cell-nanowire interaction studies,” *Small*, vol. 9, no. 2, pp. 263–272, Jan. 2013, doi: 10.1002/smll.201201314.
- [16] T. Berthing *et al.*, “Cell membrane conformation at vertical nanowire array interface revealed by fluorescence imaging,” *Nanotechnology*, vol. 23, no. 41, p. 415102, Oct. 2012, doi: 10.1088/0957-4484/23/41/415102.
- [17] W. Zhao *et al.*, “Nanoscale manipulation of membrane curvature for probing endocytosis in live cells,” *Nat Nanotechnol*, vol. 12, no. 8, pp. 750–756, Aug. 2017, doi: 10.1038/nnano.2017.98.
- [18] S. Gopal *et al.*, “Porous Silicon Nanoneedles Modulate Endocytosis to Deliver Biological Payloads,” *Advanced Materials*, vol. 31, no. 12, p. 1806788, 2019, doi: 10.1002/adma.201806788.
- [19] J. J. VanDersarl, A. M. Xu, and N. A. Melosh, “Nanostraws for Direct Fluidic Intracellular Access,” *Nano Lett.*, vol. 12, no. 8, pp. 3881–3886, Aug. 2012, doi: 10.1021/nl204051v.
- [20] A. M. Xu *et al.*, “Quantification of nanowire penetration into living cells,” *Nat Commun*, vol. 5, no. 1, Art. no. 1, Apr. 2014, doi: 10.1038/ncomms4613.
- [21] X. Xie, A. M. Xu, S. Leal-Ortiz, Y. Cao, C. C. Garner, and N. A. Melosh, “Nanostraw-electroporation system for highly efficient intracellular delivery and transfection,” *ACS Nano*, vol. 7, no. 5, pp. 4351–4358, May 2013, doi: 10.1021/nn400874a.
- [22] E. Hebisch, M. Hjort, D. Volpati, and C. N. Prinz, “Nanostraw-Assisted Cellular Injection of Fluorescent Nanodiamonds via Direct Membrane Opening,” *Small*, vol. 17, no. 7, p. e2006421, Feb. 2021, doi: 10.1002/smll.202006421.
- [23] R. Parameswaran *et al.*, “Photoelectrochemical modulation of neuronal activity with free-standing coaxial silicon nanowires,” *Nat Nanotechnol*, vol. 13, no. 3, pp. 260–266, Mar. 2018, doi: 10.1038/s41565-017-0041-7.
- [24] B. He, T. J. Morrow, and C. D. Keating, “Nanowire sensors for multiplexed detection of biomolecules,” *Curr Opin Chem Biol*, vol. 12, no. 5, pp. 522–528, Oct. 2008, doi: 10.1016/j.cbpa.2008.08.027.
- [25] F. Patolsky, G. Zheng, and C. M. Lieber, “Nanowire sensors for medicine and the life sciences,” *Nanomedicine (Lond)*, vol. 1, no. 1, pp. 51–65, Jun. 2006, doi: 10.2217/17435889.1.1.51.

- [26] Y. Cui, Q. Wei, H. Park, and C. M. Lieber, "Nanowire nanosensors for highly sensitive and selective detection of biological and chemical species," *Science*, vol. 293, no. 5533, pp. 1289–1292, Aug. 2001, doi: 10.1126/science.1062711.
- [27] F. Patolsky, G. Zheng, O. Hayden, M. Lakadamyali, X. Zhuang, and C. M. Lieber, "Electrical detection of single viruses," *Proc Natl Acad Sci U S A*, vol. 101, no. 39, pp. 14017–14022, Sep. 2004, doi: 10.1073/pnas.0406159101.
- [28] D. Sadighbayan, M. Hasanzadeh, and E. Ghafar-Zadeh, "Biosensing based on field-effect transistors (FET): Recent progress and challenges," *TrAC Trends in Analytical Chemistry*, vol. 133, p. 116067, Dec. 2020, doi: 10.1016/j.trac.2020.116067.
- [29] N. Gao *et al.*, "Specific detection of biomolecules in physiological solutions using graphene transistor biosensors," *Proceedings of the National Academy of Sciences*, vol. 113, no. 51, pp. 14633–14638, Dec. 2016, doi: 10.1073/pnas.1625010114.
- [30] X. Duan *et al.*, "Intracellular recordings of action potentials by an extracellular nanoscale field-effect transistor," *Nat Nanotechnol*, vol. 7, no. 3, pp. 174–179, Dec. 2011, doi: 10.1038/nnano.2011.223.
- [31] A. Dorfman, N. Kumar, and J. Hahm, "Highly sensitive biomolecular fluorescence detection using nanoscale ZnO platforms," *Langmuir*, vol. 22, no. 11, pp. 4890–4895, May 2006, doi: 10.1021/la053270+.
- [32] M. Lard, H. Linke, and C. N. Prinz, "Biosensing using arrays of vertical semiconductor nanowires: mechanosensing and biomarker detection," *Nanotechnology*, vol. 30, no. 21, p. 214003, Mar. 2019, doi: 10.1088/1361-6528/ab0326.
- [33] W. Hu, Y. Liu, H. Yang, X. Zhou, and C. M. Li, "ZnO nanorods-enhanced fluorescence for sensitive microarray detection of cancers in serum without additional reporter-amplification," *Biosens Bioelectron*, vol. 26, no. 8, pp. 3683–3687, Apr. 2011, doi: 10.1016/j.bios.2011.01.045.
- [34] L. ten Siethoff, M. Lard, J. Generosi, H. S. Andersson, H. Linke, and A. Månsson, "Molecular Motor Propelled Filaments Reveal Light-Guiding in Nanowire Arrays for Enhanced Biosensing," *Nano Lett.*, vol. 14, no. 2, pp. 737–742, Feb. 2014, doi: 10.1021/nl404032k.
- [35] R. S. Frederiksen *et al.*, "Modulation of Fluorescence Signals from Biomolecules along Nanowires Due to Interaction of Light with Oriented Nanostructures," *Nano Lett.*, vol. 15, no. 1, pp. 176–181, Jan. 2015, doi: 10.1021/nl503344y.
- [36] D. Verardo *et al.*, "Nanowires for Biosensing: Lightguiding of Fluorescence as a Function of Diameter and Wavelength," *Nano Lett*, vol. 18, no. 8, pp. 4796–4802, Aug. 2018, doi: 10.1021/acs.nanolett.8b01360.
- [37] R. S. Frederiksen *et al.*, "Nanowire-Aperture Probe: Local Enhanced Fluorescence Detection for the Investigation of Live Cells at the Nanoscale," *ACS Photonics*, vol. 3, no. 7, pp. 1208–1216, Jul. 2016, doi: 10.1021/acsp Photonics.6b00126.
- [38] D. Verardo *et al.*, "Fluorescence Signal Enhancement in Antibody Microarrays Using Lightguiding Nanowires," *Nanomaterials (Basel)*, vol. 11, no. 1, p. 227, Jan. 2021, doi: 10.3390/nano11010227.

- [39] G. Russo, C. Zegar, and A. Giordano, “Advantages and limitations of microarray technology in human cancer,” *Oncogene*, vol. 22, no. 42, pp. 6497–6507, Sep. 2003, doi: 10.1038/sj.onc.1206865.
- [40] P. Trayhurn, “Northern blotting,” *Proc Nutr Soc*, vol. 55, no. 1B, pp. 583–589, Mar. 1996, doi: 10.1079/pns19960051.
- [41] K. Polyak and M. Meyerson, “Gene Expression: MRNA Transcript Analysis,” in *Holland-Frei Cancer Medicine. 6th edition*, BC Decker, 2003. Accessed: Nov. 13, 2023. [Online]. Available: <https://www.ncbi.nlm.nih.gov/books/NBK12777/>
- [42] “Northern and Southern Blot Protocols & Introduction.” Accessed: Nov. 14, 2023. [Online]. Available: <https://www.sigmaaldrich.com/SE/en/technical-documents/protocol/protein-biology/gel-electrophoresis/southern-and-northern-blotting>
- [43] T. Yang, M. Zhang, and N. Zhang, “Modified Northern blot protocol for easy detection of mRNAs in total RNA using radiolabeled probes,” *BMC Genomics*, vol. 23, no. 1, p. 66, Jan. 2022, doi: 10.1186/s12864-021-08275-w.
- [44] Z. Dvorák, J.-M. Pascussi, and M. Modrianský, “Approaches to messenger RNA detection - comparison of methods,” *Biomed Pap Med Fac Univ Palacky Olomouc Czech Repub*, vol. 147, no. 2, pp. 131–135, Dec. 2003, doi: 10.5507/bp.2003.018.
- [45] Y. J. Ma, G. A. Dissen, F. Rage, and S. R. Ojeda, “RNase Protection Assay,” *Methods*, vol. 10, no. 3, pp. 273–278, Dec. 1996, doi: 10.1006/meth.1996.0102.
- [46] “The Basics: Nuclease Protection Assays - SE.” Accessed: Nov. 13, 2023. [Online]. Available: <https://www.thermofisher.com/uk/en/home/references/ambion-tech-support/ribonuclease-protection-assays/general-articles/the-basics-what-is-a-nuclease-protection-assay.html>
- [47] J. B. Rottman, “The Ribonuclease Protection Assay: A Powerful Tool for the Veterinary Pathologist,” *Vet Pathol*, vol. 39, no. 1, pp. 2–9, Jan. 2002, doi: 10.1354/vp.39-1-2.
- [48] E. Jensen, “Technical Review: In Situ Hybridization,” *The Anatomical Record*, vol. 297, no. 8, pp. 1349–1353, 2014, doi: 10.1002/ar.22944.
- [49] S. Higo, H. Ishii, and H. Ozawa, “Recent Advances in High-sensitivity In Situ Hybridization and Costs and Benefits to Consider When Employing These Methods,” *Acta Histochem Cytochem*, vol. 56, no. 3, pp. 49–54, Jun. 2023, doi: 10.1267/ahc.23-00024.
- [50] C. J. Smith and A. M. Osborn, “Advantages and limitations of quantitative PCR (Q-PCR)-based approaches in microbial ecology,” *FEMS Microbiol Ecol*, vol. 67, no. 1, pp. 6–20, Jan. 2009, doi: 10.1111/j.1574-6941.2008.00629.x.
- [51] Y. Wang and N. E. Navin, “Advances and Applications of Single Cell Sequencing Technologies,” *Physiology & behavior*, vol. 176, no. 1, pp. 139–148, 2016, doi: 10.1016/j.molcel.2015.05.005.Advances.
- [52] A. K. Chen, M. A. Behlke, and A. Tsourkas, “Avoiding false-positive signals with nuclease-vulnerable molecular beacons in single living cells,” *Nucleic Acids Res*, vol. 35, no. 16, p. e105, 2007, doi: 10.1093/nar/gkm593.

- [53] X. L. Gao, M. Zhang, Y. L. Tang, and X. H. Liang, "Cancer cell dormancy: Mechanisms and implications of cancer recurrence and metastasis," *OncoTargets and Therapy*, vol. 10, pp. 5219–5228, 2017, doi: 10.2147/OTT.S140854.
- [54] T. Kuang, L. Chang, X. Peng, X. Hu, and D. Gallego-Perez, "Molecular Beacon Nano-Sensors for Probing Living Cancer Cells," *Trends in Biotechnology*, vol. 35, no. 4, pp. 347–359, 2017, doi: 10.1016/j.tibtech.2016.09.003.
- [55] J. G. Carlton, H. Jones, and U. S. Eggert, "Membrane and organelle dynamics during cell division," *Nat Rev Mol Cell Biol*, vol. 21, no. 3, pp. 151–166, Mar. 2020, doi: 10.1038/s41580-019-0208-1.
- [56] D. A. Guertin, S. Trautmann, and D. McCollum, "Cytokinesis in eukaryotes," *Microbiol Mol Biol Rev*, vol. 66, no. 2, pp. 155–178, Jun. 2002, doi: 10.1128/MMBR.66.2.155-178.2002.
- [57] T. Oki *et al.*, "A novel cell-cycle-indicator, mVenus-p27K-, identifies quiescent cells and visualizes G0-G1 transition," *Sci Rep*, vol. 4, p. 4012, Feb. 2014, doi: 10.1038/srep04012.
- [58] X. Gao, M. Zhang, Y. Tang, and X. Liang, "Cancer cell dormancy: mechanisms and implications of cancer recurrence and metastasis," *Onco Targets Ther*, vol. 10, pp. 5219–5228, Oct. 2017, doi: 10.2147/OTT.S140854.
- [59] S.-Y. Park and J.-S. Nam, "The force awakens: metastatic dormant cancer cells," *Exp Mol Med*, vol. 52, no. 4, Art. no. 4, Apr. 2020, doi: 10.1038/s12276-020-0423-z.
- [60] M. P. F. Damen, J. van Rheenen, and C. L. G. J. Scheele, "Targeting dormant tumor cells to prevent cancer recurrence," *FEBS J*, vol. 288, no. 21, pp. 6286–6303, Nov. 2021, doi: 10.1111/febs.15626.
- [61] H. Wang and X. He, "Nanoparticles for Targeted Drug Delivery to Cancer Stem Cells and Tumor," *Methods Mol Biol*, vol. 1831, pp. 59–67, 2018, doi: 10.1007/978-1-4939-8661-3_6.
- [62] G. Otnes and M. T. Borgström, "Towards high efficiency nanowire solar cells," *Nano Today*, vol. 12, pp. 31–45, Feb. 2017, doi: 10.1016/j.nantod.2016.10.007.
- [63] W. Lu and C. M. Lieber, "Semiconductor nanowires," *J. Phys. D: Appl. Phys.*, vol. 39, no. 21, p. R387, Oct. 2006, doi: 10.1088/0022-3727/39/21/R01.
- [64] Y. Qu and X. Duan, "One-dimensional homogeneous and heterogeneous nanowires for solar energy conversion," *J. Mater. Chem.*, vol. 22, no. 32, pp. 16171–16181, Jul. 2012, doi: 10.1039/C2JM32267F.
- [65] F. Zafar and A. Iqbal, "Indium phosphide nanowires and their applications in optoelectronic devices," *Proceedings of the Royal Society A: Mathematical, Physical and Engineering Sciences*, vol. 472, no. 2187, p. 20150804, Mar. 2016, doi: 10.1098/rspa.2015.0804.
- [66] E. Barrigón, M. Heurlin, Z. Bi, B. Monemar, and L. Samuelson, "Synthesis and Applications of III–V Nanowires," *Chem. Rev.*, vol. 119, no. 15, pp. 9170–9220, Aug. 2019, doi: 10.1021/acs.chemrev.9b00075.
- [67] A. R. Frederickson and P. Rabkin, "Simple model for carrier densities in the depletion region of p-n junctions," *IEEE Transactions on Electron Devices*, vol. 40, no. 5, pp. 994–1000, May 1993, doi: 10.1109/16.210210.

- [68] G. Otnes and M. T. Borgström, “Towards high efficiency nanowire solar cells,” *Nano Today*, vol. 12, pp. 31–45, 2017, doi: 10.1016/j.nantod.2016.10.007.
- [69] K. Y. Baik *et al.*, “Synthetic nanowire/nanotube-based solid substrates for controlled cell growth,” *Nano Convergence*, vol. 1, no. 1, pp. 1–10, 2014, doi: 10.1186/s40580-014-0028-0.
- [70] S. Bonde *et al.*, “Tuning InAs nanowire density for HEK293 cell viability, adhesion, and morphology: Perspectives for nanowire-based biosensors,” *ACS Applied Materials and Interfaces*, vol. 5, no. 21, pp. 10510–10519, 2013, doi: 10.1021/am402070k.
- [71] Z. Li, H. Persson, K. Adolffson, S. Oredsson, and C. N. Prinz, “Morphology of living cells cultured on nanowire arrays with varying nanowire densities and diameters,” *Science China Life Sciences*, vol. 61, no. 4, pp. 427–435, 2018, doi: 10.1007/s11427-017-9264-2.
- [72] M. Dipalo *et al.*, “Cells Adhering to 3D Vertical Nanostructures: Cell Membrane Reshaping without Stable Internalization,” *Nano Letters*, vol. 18, no. 9, pp. 6100–6105, 2018, doi: 10.1021/acs.nanolett.8b03163.
- [73] N. Buch-Månson, D. H. Kang, D. Kim, K. E. Lee, M. H. Yoon, and K. L. Martinez, “Mapping cell behavior across a wide range of vertical silicon nanocolumn densities,” *Nanoscale*, vol. 9, no. 17, pp. 5517–5527, 2017, doi: 10.1039/c6nr09700f.
- [74] H. Persson, Z. Li, J. O. Tegenfeldt, S. Oredsson, and C. N. Prinz, “From immobilized cells to motile cells on a bed-of-nails: Effects of vertical nanowire array density on cell behaviour,” *Scientific Reports*, vol. 5, no. July, pp. 1–12, 2015, doi: 10.1038/srep18535.
- [75] D. Zhao *et al.*, “Single-molecule detection and tracking of RNA transcripts in living cells using phosphorothioate-optimized 2'-O-methyl RNA molecular beacons,” *Biomaterials*, vol. 100, pp. 172–183, 2016, doi: 10.1016/j.biomaterials.2016.05.022.
- [76] R. Monroy-Contreras and L. Vaca, “Molecular beacons: Powerful tools for imaging RNA in living cells,” *Journal of Nucleic Acids*, vol. 2011, 2011, doi: 10.4061/2011/741723.
- [77] M. Chen *et al.*, “A molecular beacon-based approach for live-cell imaging of RNA transcripts with minimal target engineering at the single-molecule level,” *Scientific Reports*, vol. 7, no. 1, pp. 1–11, 2017, doi: 10.1038/s41598-017-01740-1.
- [78] D. Y. Ryazantsev *et al.*, “Design of molecular beacons: 3' couple quenchers improve fluorogenic properties of a probe in real-time PCR assay,” *Analyst*, vol. 139, no. 11, pp. 2867–2872, 2014, doi: 10.1039/c4an00081a.
- [79] S. Tyagi and F. R. Kramer, “Molecular beacons in diagnostics,” *F1000 Medicine Reports*, vol. 4, no. 1, pp. 2–7, 2012, doi: 10.3410/M4-10.
- [80] G. Goel, A. Kumar, A. K. Puniya, W. Chen, and K. Singh, “Molecular beacon: A multitask probe,” *Journal of Applied Microbiology*, vol. 99, no. 3, pp. 435–442, 2005, doi: 10.1111/j.1365-2672.2005.02663.x.
- [81] T. J. Drake and W. Tan, “Molecular Beacon DNA Probes and their Bioanalytical Applications,” *Applied Spectroscopy*, vol. 58, no. 9, pp. 269–280, 2004.

- [82] S. X. Han, X. Jia, J. L. Ma, and Q. Zhu, "Molecular beacons: A novel optical diagnostic tool," *Archivum Immunologiae et Therapiae Experimentalis*, vol. 61, no. 2, pp. 139–148, 2013, doi: 10.1007/s00005-012-0209-7.
- [83] J. Perlette and W. Tan, "Real-time monitoring of intracellular mRNA hybridization inside single living cells," *Anal Chem*, vol. 73, no. 22, pp. 5544–5550, Nov. 2001, doi: 10.1021/ac010633b.
- [84] W. J. Rhee and G. Bao, "Slow non-specific accumulation of 2'-deoxy and 2'-O-methyl oligonucleotide probes at mitochondria in live cells," *Nucleic Acids Res*, vol. 38, no. 9, p. e109, May 2010, doi: 10.1093/nar/gkq050.
- [85] Q. Ding, Q. Zhan, X. Zhou, T. Zhang, and D. Xing, "Theranostic Upconversion Nanobeacons for Tumor mRNA Ratiometric Fluorescence Detection and Imaging-Monitored Drug Delivery," *Small*, vol. 12, no. 43, pp. 5944–5953, Nov. 2016, doi: 10.1002/smll.201601724.
- [86] D. Zhao *et al.*, "Single-molecule detection and tracking of RNA transcripts in living cells using phosphorothioate-optimized 2'-O-methyl RNA molecular beacons," *Biomaterials*, vol. 100, pp. 172–183, Sep. 2016, doi: 10.1016/j.biomaterials.2016.05.022.
- [87] S. Tyagi and O. Alsmadi, "Imaging Native β -Actin mRNA in Motile Fibroblasts," *Biophys J*, vol. 87, no. 6, pp. 4153–4162, Dec. 2004, doi: 10.1529/biophysj.104.045153.
- [88] A. K. Chen, M. A. Behlke, and A. Tsourkas, "Efficient cytosolic delivery of molecular beacon conjugates and flow cytometric analysis of target RNA," *Nucleic Acids Research*, vol. 36, no. 12, 2008, doi: 10.1093/nar/gkn331.
- [89] N. Nitin, P. J. Santangelo, G. Kim, S. Nie, and G. Bao, "Peptide-linked molecular beacons for efficient delivery and rapid mRNA detection in living cells.," *Nucleic acids research*, vol. 32, no. 6, pp. 1–8, 2004, doi: 10.1093/nar/gnh063.
- [90] D. P. Bratu, B. J. Cha, M. M. Mhlanga, F. R. Kramer, and S. Tyagi, "Visualizing the distribution and transport of mRNAs in living cells," *Proceedings of the National Academy of Sciences of the United States of America*, vol. 100, no. 23, pp. 13308–13313, 2003, doi: 10.1073/pnas.2233244100.
- [91] Y. T. Chow *et al.*, "Single Cell Transfection through Precise Microinjection with Quantitatively Controlled Injection Volumes," *Sci Rep*, vol. 6, p. 24127, Apr. 2016, doi: 10.1038/srep24127.
- [92] M. Chen *et al.*, "A molecular beacon-based approach for live-cell imaging of RNA transcripts with minimal target engineering at the single-molecule level," *Sci Rep*, vol. 7, no. 1, p. 1550, May 2017, doi: 10.1038/s41598-017-01740-1.
- [93] D. P. Bratu, B.-J. Cha, M. M. Mhlanga, F. R. Kramer, and S. Tyagi, "Visualizing the distribution and transport of mRNAs in living cells," *Proc Natl Acad Sci U S A*, vol. 100, no. 23, pp. 13308–13313, Nov. 2003, doi: 10.1073/pnas.2233244100.
- [94] X. Xie, A. M. Xu, S. Leal-Ortiz, Y. Cao, C. C. Garner, and N. A. Melosh, "Nanostraw-electroporation system for highly efficient intracellular delivery and transfection," *ACS Nano*, vol. 7, no. 5, pp. 4351–4358, 2013, doi: 10.1021/nn400874a.

- [95] L. Schmiderer *et al.*, “Efficient and nontoxic biomolecule delivery to primary human hematopoietic stem cells using nanostraws,” *Proc Natl Acad Sci U S A*, vol. 117, no. 35, pp. 21267–21273, Sep. 2020, doi: 10.1073/pnas.2001367117.
- [96] Y. Cao *et al.*, “Universal intracellular biomolecule delivery with precise dosage control,” *Sci Adv*, vol. 4, no. 10, p. eaat8131, Oct. 2018, doi: 10.1126/sciadv.aat8131.
- [97] Y. Cao *et al.*, “Nondestructive nanostraw intracellular sampling for longitudinal cell monitoring,” *Proc Natl Acad Sci U S A*, vol. 114, no. 10, pp. E1866–E1874, Mar. 2017, doi: 10.1073/pnas.1615375114.
- [98] C. Situma, A. J. Moehring, M. A. F. Noor, and S. A. Soper, “Immobilized molecular beacons: a new strategy using UV-activated poly(methyl methacrylate) surfaces to provide large fluorescence sensitivities for reporting on molecular association events,” *Anal Biochem*, vol. 363, no. 1, pp. 35–45, Apr. 2007, doi: 10.1016/j.ab.2006.12.029.
- [99] Á. Ruiz-Tórtola *et al.*, “High sensitivity and label-free oligonucleotides detection using photonic bandgap sensing structures biofunctionalized with molecular beacon probes,” *Biomed Opt Express*, vol. 9, no. 4, pp. 1717–1727, Apr. 2018, doi: 10.1364/BOE.9.001717.
- [100] H. Du, C. M. Strohsahl, J. Camera, B. L. Miller, and T. D. Krauss, “Sensitivity and Specificity of Metal Surface-Immobilized ‘Molecular Beacon’ Biosensors,” *J. Am. Chem. Soc.*, vol. 127, no. 21, pp. 7932–7940, Jun. 2005, doi: 10.1021/ja042482a.
- [101] Y. Moon, H. Moon, J. Chang, H. D. Kim, J. H. Lee, and J. Lee, “Development of a highly sensitive lateral flow strip device for nucleic acid detection using molecular beacons,” *Frontiers in Sensors*, vol. 3, 2022, Accessed: Sep. 04, 2023. [Online]. Available: <https://www.frontiersin.org/articles/10.3389/fsens.2022.1012775>
- [102] H. Ma, K. N. Bell, and R. N. Loker, “qPCR and qRT-PCR analysis: Regulatory points to consider when conducting biodistribution and vector shedding studies,” *Molecular Therapy - Methods & Clinical Development*, vol. 20, pp. 152–168, Mar. 2021, doi: 10.1016/j.omtm.2020.11.007.
- [103] J. J. Li, Y. Chu, B. Y.-H. Lee, and X. S. Xie, “Enzymatic signal amplification of molecular beacons for sensitive DNA detection,” *Nucleic Acids Res*, vol. 36, no. 6, p. e36, Apr. 2008, doi: 10.1093/nar/gkn033.
- [104] D. van Dam *et al.*, “Directional and Polarized Emission from Nanowire Arrays,” *Nano Lett*, vol. 15, no. 7, pp. 4557–4563, Jul. 2015, doi: 10.1021/acs.nanolett.5b01135.
- [105] J. Valderas-Gutiérrez *et al.*, “Enhanced Optical Biosensing by Aerotaxy Ga(As)P Nanowire Platforms Suitable for Scalable Production,” *ACS Appl Nano Mater*, vol. 5, no. 7, pp. 9063–9071, Jul. 2022, doi: 10.1021/acsnm.2c01372.
- [106] K. B. Cederquist and C. D. Keating, “Hybridization Efficiency of Molecular Beacons Bound to Gold Nanowires: Effect of Surface Coverage and Target Length,” *Langmuir*, vol. 26, no. 23, pp. 18273–18280, Dec. 2010, doi: 10.1021/la1031703.
- [107] X. Liu and W. Tan, “A fiber-optic evanescent wave DNA biosensor based on novel molecular beacons,” *Anal Chem*, vol. 71, no. 22, pp. 5054–5059, Nov. 1999, doi: 10.1021/ac990561c.

- [108] H. Du, M. D. Disney, B. L. Miller, and T. D. Krauss, "Hybridization-based unquenching of DNA hairpins on au surfaces: prototypical 'molecular beacon' biosensors," *J Am Chem Soc*, vol. 125, no. 14, pp. 4012–4013, Apr. 2003, doi: 10.1021/ja0290781.
- [109] F. Zafar and A. Iqbal, "Indium phosphide nanowires and their applications in optoelectronic devices," *Proceedings of the Royal Society A: Mathematical, Physical and Engineering Sciences*, vol. 472, no. 2187, 2016, doi: 10.1098/rspa.2015.0804.
- [110] P. O. Oviroh, R. Akbarzadeh, D. Pan, R. A. M. Coetzee, and T. C. Jen, "New development of atomic layer deposition: processes, methods and applications," *Science and Technology of Advanced Materials*, vol. 20, no. 1, pp. 465–496, 2019, doi: 10.1080/14686996.2019.1599694.
- [111] R. W. Johnson, A. Hultqvist, and S. F. Bent, "A brief review of atomic layer deposition: From fundamentals to applications," *Materials Today*, vol. 17, no. 5, pp. 236–246, 2014, doi: 10.1016/j.mattod.2014.04.026.
- [112] E. McCafferty and J. P. Wightman, "Determination of the concentration of surface hydroxyl groups on metal oxide films by a quantitative XPS method," *Surface and Interface Analysis*, vol. 26, no. 8, pp. 549–564, 1998, doi: 10.1002/(sici)1096-9918(199807)26:8<549::aid-sia396>3.3.co;2-h.
- [113] S. E. Potts, W. Keuning, E. Langereis, G. Dingemans, M. C. M. van de Sanden, and W. M. M. Kessels, "Low Temperature Plasma-Enhanced Atomic Layer Deposition of Metal Oxide Thin Films," *Journal of The Electrochemical Society*, vol. 157, no. 7, p. P66, 2010, doi: 10.1149/1.3428705.
- [114] Z. Zhu *et al.*, "Low-Temperature Plasma-Enhanced Atomic Layer Deposition of SiO₂ Using Carbon Dioxide," *Nanoscale Research Letters*, vol. 14, 2019, doi: 10.1186/s11671-019-2889-y.
- [115] Q. Xing, "Information or resolution: Which is required from an SEM to study bulk inorganic materials?," *Scanning*, vol. 38, no. 6, pp. 864–879, 2016, doi: 10.1002/sca.21336.
- [116] M. J. Park, D. H. Kim, K. Park, D. Y. Jang, and D. C. Han, "Design and fabrication of a scanning electron microscope using a finite element analysis for electron optical system," *Journal of Mechanical Science and Technology*, vol. 22, no. 9, pp. 1734–1746, 2008, doi: 10.1007/s12206-008-0317-9.
- [117] H. Seiler, "Secondary electron emission in the scanning electron microscope," *Journal of Applied Physics*, vol. 54, no. 11, 1983, doi: 10.1063/1.332840.
- [118] P. Kejzlar, M. Švec, and E. Macajová, "The usage of backscattered electrons in scanning electron microscopy," *Manufacturing Technology*, vol. 14, no. 3, pp. 333–336, 2014, doi: 10.21062/ujep/x.2014/a/1213-2489/mt/14/3/333.
- [119] R. Zhou *et al.*, "Understanding and optimizing EBIC pn-junction characterization from modeling insights," *Journal of Applied Physics*, vol. 127, no. 2, 2020, doi: 10.1063/1.5139894.
- [120] H. J. Leamy, "Charge collection scanning electron microscopy," *Journal of Applied Physics*, vol. 53, no. 6, 1982, doi: 10.1063/1.331667.

- [121] H. E. Hohmeier, H. Mulder, G. Chen, R. Henkel-Rieger, M. Prentki, and C. B. Newgard, "Isolation of INS-1-derived cell lines with robust ATP-sensitive K⁺ channel-dependent and -independent glucose-stimulated insulin secretion," *Diabetes*, vol. 49, no. 3, pp. 424–430, Mar. 2000, doi: 10.2337/diabetes.49.3.424.
- [122] M. J. Sanderson, I. Smith, I. Parker, and M. D. Bootman, "Fluorescence Microscopy," *Cold Spring Harb Protoc*, vol. 2014, no. 10, p. pdb.top071795, Oct. 2014, doi: 10.1101/pdb.top071795.
- [123] L. T. Li, G. Jiang, Q. Chen, and J. N. Zheng, "Ki67 is a promising molecular target in the diagnosis of cancer (review)," *Mol Med Rep*, vol. 11, no. 3, pp. 1566–1572, Mar. 2015, doi: 10.3892/mmr.2014.2914.
- [124] S. Elmore, "Apoptosis: A Review of Programmed Cell Death," *Toxicol Pathol*, vol. 35, no. 4, pp. 495–516, 2007, doi: 10.1080/01926230701320337.
- [125] Z. Darzynkiewicz, D. Galkowski, and H. Zhao, "Analysis of apoptosis by cytometry using TUNEL assay," *Methods*, vol. 44, no. 3, pp. 250–254, 2008, doi: 10.1016/j.ymeth.2007.11.008.
- [126] G. M. Cooper, "Lysosomes," in *The Cell: A Molecular Approach. 2nd edition*, Sinauer Associates, 2000. Accessed: Nov. 02, 2023. [Online]. Available: <https://www.ncbi.nlm.nih.gov/books/NBK9953/>
- [127] B. Zhitomirsky, H. Farber, and Y. G. Assaraf, "LysoTracker and MitoTracker Red are transport substrates of P-glycoprotein: implications for anticancer drug design evading multidrug resistance," *J Cell Mol Med*, vol. 22, no. 4, pp. 2131–2141, Apr. 2018, doi: 10.1111/jcmm.13485.
- [128] J. Bucevičius, G. Lukinavičius, and R. Gerasimaitė, "The Use of Hoechst Dyes for DNA Staining and Beyond," *Chemosensors*, vol. 6, no. 2, Art. no. 2, Jun. 2018, doi: 10.3390/chemosensors6020018.
- [129] "National Center for Biotechnology Information." Accessed: Apr. 16, 2021. [Online]. Available: <https://www.ncbi.nlm.nih.gov/>
- [130] "Rattus norvegicus insulin 1 (Ins1), mRNA - Nucleotide - NCBI." Accessed: Apr. 16, 2021. [Online]. Available: https://www.ncbi.nlm.nih.gov/nucleotide/NM_019129.3
- [131] "RNAfold web server." Accessed: Sep. 04, 2023. [Online]. Available: <http://rna.tbi.univie.ac.at/cgi-bin/RNAWebSuite/RNAfold.cgi>
- [132] "BLAST: Basic Local Alignment Search Tool." Accessed: Apr. 16, 2021. [Online]. Available: <https://blast.ncbi.nlm.nih.gov/Blast.cgi>
- [133] "Freiburg RNA Tools." Accessed: Apr. 16, 2021. [Online]. Available: <http://rna.informatik.uni-freiburg.de/>
- [134] "Integrated DNA Technologies | IDT," Integrated DNA Technologies. Accessed: Sep. 04, 2023. [Online]. Available: <https://eu.idtdna.com/pages>
- [135] J. C. McDonald and G. M. Whitesides, "Poly(dimethylsiloxane) as a material for fabricating microfluidic devices," *Acc Chem Res*, vol. 35, no. 7, pp. 491–499, Jul. 2002, doi: 10.1021/ar010110q.
- [136] H. Endo and M. Inoue, "Dormancy in cancer," *Cancer Sci*, vol. 110, no. 2, pp. 474–480, Feb. 2019, doi: 10.1111/cas.13917.

- [137] A. Weintraub, "Preventing cancer metastasis by keeping dormant tumor cells asleep with collagen," Fierce Biotech. Accessed: Nov. 16, 2023. [Online]. Available: <https://www.fiercebitech.com/research/preventing-cancer-metastasis-by-keeping-dormant-tumor-cells-asleep-collagen>
- [138] A. K. Chen, M. A. Behlke, and A. Tsourkas, "Sub-cellular trafficking and functionality of 2'- O -methyl and 2'- O -methyl-phosphorothioate molecular beacons," *Nucleic Acids Research*, vol. 37, no. 22, p. e149, Dec. 2009, doi: 10.1093/nar/gkp837.
- [139] L. Yang *et al.*, "A Highly Sensitive Strategy for Fluorescence Imaging of MicroRNA in Living Cells and in Vivo Based on Graphene Oxide-Enhanced Signal Molecules Quenching of Molecular Beacon," *ACS Appl Mater Interfaces*, vol. 10, no. 8, pp. 6982–6990, Feb. 2018, doi: 10.1021/acsami.7b19284.
- [140] C. Xing *et al.*, "Accelerated DNA tetrahedron-based molecular beacon for efficient microRNA imaging in living cells," *Chem. Commun.*, vol. 57, no. 26, pp. 3251–3254, Mar. 2021, doi: 10.1039/D0CC08172H.

